2011

PROTEOMIC ANALYSIS OF TWO DIFFERENT STATES OF NAEGLERIA FOWLERI

Hong Park
Virginia Commonwealth University

PROTEOMIC ANALYSIS OF TWO DIFFERENT STATES OF *NAEGLERIA FOWLERI*

A Thesis submitted in partial fulfillment of the requirements for the degree of Master of Science at Virginia Commonwealth University.

by

HONG GEUN PARK

Bachelor of Science, University of Virginia, 2009

Director: DR. GUY A. CABRAL, PH.D.

PROFESSOR, DEPARTMENT OF MICROBIOLOGY AND IMMUNOLOGY

Virginia Commonwealth University
Richmond, Virginia
August, 2013

Acknowledgements

I would like to extend my deep gratitude to the following individuals for their support and encouragement throughout my graduate career. Without their assistance I would not be where I am today. First and most importantly I would like to thank Dr. Guy Cabral for accepting me into his lab and his constant guidance and encouragement. He has been a wonderful role model and mentor and has taught me a great deal about passion for one's work. I would also like to thank Dr. Francine Marciano-Cabral for her knowledge and advice that she has given me in this past year; they were pivotal to my success.

In addition, I would also like to thank my committee member, Dr. Darrel Peterson, for his valuable inputs and the help he provided to complete my project.

I would like to thank Dr. Melissa Jamerson for her insight and guidance. She has been an excellent teacher, and many times she went out of her way to help me. I owe a great amount of my graduate success to her. I would like to thank my fellow laboratory members and colleagues including Dr. Gabriela Ferreira, Dr. Erinn Raborn, Johnathan Drevik, and Rebecca Maddux for their continued support.

I am grateful to my parents, Jong and Sun, my brother, Jeff, for their love and emotional support throughout my life and graduate school. I'd also like to express my deepest appreciation to my friends for their support.

Table of Contents

List of Tables

Page

List of Figures

Page

Abstract

PROTEOMIC ANALYSIS OF TWO DIFFERENT STATES

OR STRAINS OF N. FOWLERI

By Hong Geun Park

A Thesis submitted in partial fulfillment of the requirements for the degree of Master of Science at Virginia Commonwealth University.

Virginia Commonwealth University, 2013.

Major Director: Dr. Guy A. Cabral, PhD.

Professor, Department of Microbiology and Immunology

Naegleria fowleri are free-living ameboflagellates found in soil and freshwater habitats throughout the world that cause a fatal disease in humans called Primary Amoebic Meningoencephalitis (PAM). Mechanisms of host resistance or susceptibility to infection have not been fully elucidated, and possible treatment methods are still sub optimal. The disease is diagnosed using specific laboratory tests available in only a few laboratories in the United States. Because of the rarity of infection and difficulty in initial detection, more than often PAM is misdiagnosed. Therefore, it is very important to find causative marker for early detection of an infection. The purpose of this study is to create a proteomic signature map using two-

dimensional gel electrophoresis (2-D gel) and recommend a subset of proteins that may be directly linked to the pathogenic state of *N. fowleri*.

Replicates of 2-D Gels were created for both strains of *N. fowleri* and the proteomic templates from these gels were compared with each other. Scatter Plots were generated measuring the density of protein spots from 2-D gels being analyzed for each study. For each strains of N. fowleri, the 2-D gels from each study were compared within and compared between the two studies for reproducibility in data. The resulting correlation values for all of the Scatter Plots were greater or equal to 0.90. Finally, the representative proteomic template for axenically grown *N. fowleri* and mouse passaged *N. fowleri* were compared and the correlation value of 0.60 was observed. This confirmed our theory that these two strains or states of *N. fowleri* have very different protein expressions, and we were able to identify a subset of proteins, both over expressed and newly synthesized, that may be linked to the highly pathogenic state of *N. fowleri*.

INTRODUCTION

Naegleria species and background

The genus *Naegleria* consists of species of free-living amoeba (FLA) widely distributed in diverse habitats throughout the world such as freshwater lakes, ponds, domestic water supplies, swimming pools, thermal pools, soil, and dust (Marciano-Cabral, F., 2007; Martinez, A.J., 1997). Although, over 30 species of *Naegleria* have been isolated from environmental sources and domestic water supplies (Craun *et al.*, 2005; Jamerson *et al.*, 2009; Marciano-Cabral *et al.*, 2003; Yoder *et al.*, 2004), only one, *Naegleria fowleri,* has been linked to disease in humans (Cerva & Novak, 1968; Martinez, 1985). Two other species of *Naegleria*, *N. australiensis* and *N. italica*, have been shown to lyse tissue culture cells in vitro and are pathogenic in experimental animals but have not been associated with disease in humans (Marciano-Cabral, F.M., 1986; De Jonckheere, 2004).

Human disease caused by free-living amoebae was first reported in 1965 by Fowler and Carter, who studied four patients with primary amoebic meningoencephalitis (PAM) in South Australia (Fowler, M., 1965). Subsequently, accounts of patients with PAM within the United States were reported by Butt in Florida (Butt, C.G., 1966; Butt, C.G., 1968). A retrospective study conducted by dos Santos indicated that an epidemic of PAM had occurred in Richmond, VA., from 1951 to 1952 (Gustavo dos Santos, Neto, 1970). The term “primary amoebic

meningoencephalitis" was used first by Butt, and later by Carter, to distinguish infection of the CNS in humans by free-living amoebae such as *N. fowleri* from the rare invasion of the brain by the intestinal amoeba *Entamoeba histolytica* (Butt, C.G., 1966; Carter, R.F., 1968). Other free-living amoebae in soil and water, such as *Acanthamoeba* spp., are capable of producing a fatal CNS disease called granulomatous amoebic encephalitis (GAE) (Culbertson, C.G., 1958; Culbertson, C.G., 1971). However, *N. fowleri* is the only known species to cause PAM, a rapidly fatal disease of the central nervous system (CNS) that occurs generally in previously healthy children and young adults with a history of exposure to contaminated recreational, domestic, or environmental water sources (John, D.T., 1982; Carter, R.F., 1970).

Morphology

There are three morphological stages in the life cycle of *Naegleria* –a trophozoite, a flagellate, and a cyst (Martinez, A.J., 1985). The infective stage is the ameboid trophozoite, and during this stage the amoebae reproduce by binary fission and ingest their food (Center for Disease Control and Prevention Nov. 9. 2012; Marciano-Cabral,F., 2007). Surface structures on trophozoites, termed 'food-cups' (figure 2), are used to ingest bacteria and yeast in the environment as well as tissue in the infected host (Marciano-Cabral,F., 1988). The 'food-cups' are cytoplasmic extensions of the surface, vary in size and number depending on the species and strain of *Naegleria*, and are used to ingest bacteria, yeast cells, and cellular debris (John,D.T., 1984; John,D.T., 1985; Marciano-Cabral,F., 1988). A prolonged growth of *N. fowleri* in axenic culture *in vitro* results in attenuation of virulence while serial passage through mice restores and maintains virulence (Wong, Ming M., 1977; Whiteman,L.Y., 1989). The more virulent strains of mouse-passaged *N. fowleri* exhibit fewer 'food-cups' than do axenically grown *N. fowleri* (Marciano-Cabral,F., 1988). The flagellate stage can be observed when the trophozoite

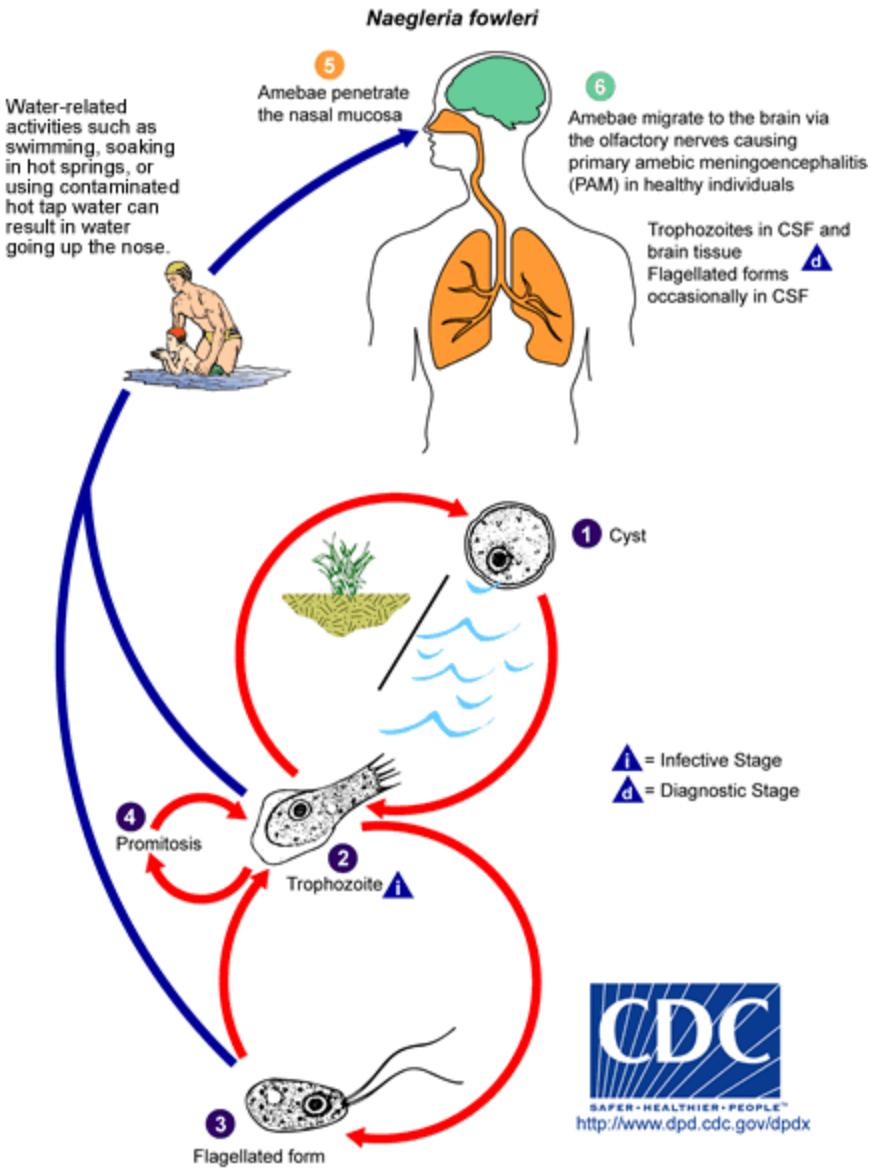

Image obtained from http://www.cdc.gov/parasites/naegleria/pathogen.html

Figure 1. Schematic representation of life cycle for *Naegleria fowleri*. *N. fowleri* has three forms including the trophozoite form which is the infective stage. Under conditions of nutrient deprivation, the trophozoite undergoes a transitory transformation to a flagellate stage, and 'swims' to the water surface to seek a bacterial food source. The cyst of *N. fowleri* affords protection from adverse environmental conditions. Factors that induce cyst formation include food deprivation, crowding, desiccation, accumulation of waste products, and exposure to toxic products of bacteria, pH changes, and salts. (Center for Disease Control and Prevention Nov. 9. 2012).

form of *N. fowleri* is incubated in non-nutrient buffer, and enflagellation process that takes several hours (Marciano-Cabral,F., 1988). When the amoebae are subjected to an unfavorable environment, such as adverse growth conditions, the trophozoite can transform into a resistant cyst form. The cyst is double-walled with a thick endocyst and a thin ectocyst. It has been proposed that the cyst stage affords protection from desiccation and food deprivation (Chang,S.L., 1978).

Primary Amebic Meningoencephalitis (PAM)

PAM typically occurs in healthy children or young adults with a recent history of swimming in lakes or pools. The disease is rapidly fatal, usually causing death within 72 hours after the onset of symptoms. Infection occurs after inhalation of water containing amebae or flagellates and then attachment to the nasal mucosa by the trophozoite form (Carter, 1972; Center for Disease Control and Prevention Nov. 9. 2012). It also has been suggested that inhaling cysts, during dusts storms, for example, could lead to infection (Lawande,R.V., 1979; Gustavo dos Santos,Neto, 1970). Amoebae penetrate the nasal mucosa and the cribiform plate and travel along the olfactory nerves to the brain. (Center for Disease Control and Prevention Nov. 9. 2012). Amoebae first invade the olfactory bulbs and then spread to the more posterior regions of the brain. Within the brain they provoke inflammation and immune response that causes extensive damage to tissue (Carter,R.F., 1970). Symptoms can be divided into two stages. Typical symptoms begin with severe frontal headache, fever, nausea, and vomiting. This series of events is followed by stiff neck, seizures, altered mental status, hallucination, and coma. Signs and symptoms of *N. fowleri* infection are clinically similar to those of bacterial meningitis, which lower the chance of initially diagnosing PAM (Yoder,J.S., 2010). PAM is considered rare, but fatal; only one person in the U.S. out of 123 has survived infection from 1962 to 2011

(Yoder,J.S., 2010). The *N. fowleri* strain obtained from the U.S. survivor did not cause damage to cells as quickly as other strains, suggesting that it is less virulent than strains recovered from other fatal cases (John,D.T., 1989; Center for Disease Control and Prevention Nov. 9. 2012). Multiple patients have received treatment similar to the California survivor, including amphotericin B, miconazole/fluconazole/ketoconazole, and/or rifampin. Several patients received almost identical treatment to the one PAM survivor but did not survive (Center for Disease Control and Prevention Nov. 9. 2012). Overall, the outlook for people who get this disease is poor, although early diagnosis and treatment might increase the chance for survival (Vargas-Zepeda,J., 2005).

Diagnostic methods

The disease is diagnosed using specific laboratory tests available in only a few laboratories in the United States. Because of the rarity of infection and difficulty in initial detection, about 75% of diagnoses are made after the death of the patient (Center for Disease Control and Prevention Nov. 9. 2012). Early diagnosis is important in order to start treatment. There are several methods for detection such as imaging, microscopic, culture, serology, and polymerase chain reaction assay can be used.

Imaging methods include Computed Tomography (CT) scans or Magnetic Resonance Imaging (MRI). These methods allow one to see the lesion, but they are nonspecific (Kidney, 1998, Schumacher,D.J., 1995). Microscopic methods include lumbar puncture, direct microscopic examination of cerebrospinal fluid (CSF), testing against polyclonal or monoclonal antibodies, and fixation of biopsy materials in formalin (Martinez,A.J., 1991, Sparagano,O., 1993). Cell Culture methods include inoculating the CSF or the biopsy tissue in tissue culture cells at 37 °C in the presence of penicillin-streptomycin. Amoebae that are present in the tissue

Survivor Medications

U.S. California Survivor [2, 3] (1978)	Mexico Survivor [4] (2003)
Amphotericin B	Amphotericin B
Rifampicin	Rifampicin
Miconazole – no longer available in US	Fluconazole
Dexamethasone	Dexamethasone
Sulfisoxazole (IV) – discontinued after *Naegleria* diagnosed	Ceftriaxone
Phenytoin	

Table 1. Medications Used by the Two Survivors. The table was adopted from the Center for Disease Control website. (http://www.cdc.gov/parasites/naegleria/treatment.html). Seidel JS et al and Vargas-Zepeda J et al have recorded the successful treatment of these patients and the table was adopted by the Center for Disease Control.

culture will multiply and destroy the monolayer of cells in 24 to 48 hours. Biopsy tissue also can be placed on 1.5% non-nutrient agar coated with a layer of bacteria (*Escherichia coli*). The amoebae will emerge from the tissue, ingest the bacteria, and divide (Martinez,A.J., 1977, Martinez,A.J., 1991, Schuster,F.L., 2002).

Two Dimension Gel Electrophoresis

Proteomics is the study of protein expression and regulation in cells, tissues, and entire organisms. Two-dimensional gel electrophoresis (2-D gel) is a cornerstone in the study of proteomics. Raw 2-D gel remains to be one of the most powerful techniques for resolving complex mixture of proteins. Using a combination of these techniques such as mass spectrometry and two dimensional gel, pharmaceutical companies may use Raw 2-D technology for high-throughput screening of drug compound candidates using protein targets.

Two-dimensional fluorescence difference gel electrophoresis (2-D DIGE) is implemented along with the 2-D Gel in order to address the gel to gel variability. The different CyDye tags have different absorption and emission spectra, which all of the samples can run on the same gel and visualized using a different excitation filters (Unlu,M., 1997). CyDye DIGE Fluors have an N-Hydroxysuccinimide (NHS) ester reactive group, which reacts with an amine group and form an amide group. The CyDye DIGE Fluors are designed to covalently attach to the epsilon amino group of lysine of proteins via an amide linkage (Unlu,M. 1997). The quantity of dye added to the sample is limiting in the reaction and approximately 1-2% of the available lysine is labeled. Thus, this method does not affect the concentration nor the size of the protein. The lysine amino acid in proteins carries a +1 charge at neutral or acidic pH. CyDye DIGE fluors also carry an intrinsic +1 charge which when coupled to the lysine, replaces the lysine's +1 charge with its

own. Ensuring that the isoelectric point (pI) of the protein does not significantly alter (Unlu,M. 1997).

Study Objective

The overall purpose of the present study is to use the proteomic approach to define specified amoebic proteins that are linked to the highly pathogenic state. The proteomic profile of highly pathogenic mouse-passaged *N. fowleri* will be compared to less pathogenic axenically grown *N. fowleri*.

Hypothesis

The hypothesis to be tested is that the differential states of mouse-passaged versus axenically-grown *N. fowleri* that have been associated with high pathogenicity versus low pathogenicity will correlate with a signature proteomic profile. Using the differential proteomic map as a fingerprint, it is proposed to identify a subset of proteins that may be linked to the high pathogenicity state.

MATERIALS AND METHODS

Naegleria cultures

N. fowleri (ATCC 30894) were obtained from the American Type Culture Collection and were grown at 37°C for 24 hours in Oxoid medium with 0.1% Hemin and 1% donor calf serum in 75 cm^2 plastic flasks (Cline *et al*., 1983). *N. foweleri* (ATCC 30894) was originally isolated from a patient who died from Primary Amebic Meningoencephalitis (PAM). A mouse-passaged strain of *N. fowleri* was maintained by introducing the strain instranasally to $B_6C_3F_1$ mice to maintain their virulence and harvested from mouse brain tissue (Toney & Marciano-Cabral, 1992). For experiments, amoebae were detached from flasks by bumping by hands and washed two times in 0.01M phosphate buffered saline (PBS), pH 7.2.

Amoeba whole-cell lysate

Amoebae grown for 24 hours with new medium were detached from tissue culture flasks, and the cell suspensions were placed in 50 mL conical tubes. The cells were washed three times in PBS. The lysis reagents was prepared (7 M Urea, 2 M Thiourea, 4% CHAPs, 30 mM Tris, 5 mM Magnesium Acetate at pH 8.5), and TBP (Tributyl phosphate), 1 uL of Endonuclease (250 units/µL) (Sigma, E8263-5KU) and 1 uL of protease inhibitor cocktail (Sigma, P8340-1ML) was added to the lysis reagent and the pellet was suspended. After suspension, the lysate solution was placed on ice for 10 min followed by sonication (ten times) at two second interval. The sonicated lysate of amoebae then was centrifuged (10 min, 12,000 x g, 4°C). The supernatant was transferred to a Spin-X filter microcentrifuge tube and centrifuged (2 min, 12,000 x g, 4°C). The sample then then was stored at -80°C overnight before assessment for protein concentration. The protein concentration was determined using the RC/DC protein assay (Biorad, Hercules, CA).

Two-Dimensional Gel Electrophoresis

First dimension starts combining 50 ug of whole cell lysate and rehydration buffer (Bio-Rad) in a microcentrifuge tube, and the final volume was adjusted to 300 uL using ReadyPrep rehydration buffer (The rehydration buffer contained includes 8 M urea (a nonionic or zwitterionic detergent), 2% CHAPS, 50 mM DTT, 0.2% Bio-Lyte® 3/10 ampholyte, 0.001% Bromophenol Blue). The adjusted mixture of whole cell lysate and rehydration buffer is then moved to a rehydration buffer tray. A 17 cm immobilized pH gradient (IPG) strip (Bio-rad, pH 5-8) was thawed (5min) and forceps were used to remove the cover. The gel portion of the strip was placed on top of the whole cell lysate and rehydration buffer mixture avoiding any air bubbles that may get trapped. The strip then was overlayed with mineral oil enough to cover one end to the other in order to avoid evaporation. The IPG strip was left on a flat surface to rehydrate over night at room temperature. Paper wicks (Bio-Rad) were dampened with ultrapure water and placed at both ends of the focusing tray channel, covering the electrodes. The mineral oil was removed from the rehydrated IPG strip and allowed to drain off of the strip by dipping the strip into a graduated cylinder filled with ultrapure water. Then the IPG strip was transferred to a focusing tray containing the dampened paper wicks. Mineral oil was overlayed again enough to cover both ends of the IPG strip. The tray was then focused using a PROTEIN IEF cell (Bio-Rad) for a total of 42,000 volt-hours. The IPG strips were removed from the focusing tray, mineral oil was allowed to drain for 10 seconds, and then transferred gel side up to a clean rehydration tray. The strip then was frozen at -80°C until needed for the second dimension.

The frozen IPG strip was thawed in room temperature for 10 minutes. The strip then was placed gel side up in a clean rehydration buffer tray and covered with Equilibration Buffer I purchased from BioRad, containing 375 mM Tris-HCL, pH 8.8, 6 M Urea, 2% DTT, and 2% SDS. The tray was placed on an shaker shaking gently for 20 minutes. At the end of the

incubation period the buffer was removed using a pipet then the IPG strip was covered with Equilibration Buffer II (BioRad), placed on a shaker for 20 minutes. The IPG strip was then dipped in a graduated cylinder containing ultrapure water and placed gel side up onto the 10% SDS-PAGE gel. Once the entire side of the IPG strip is making contact with the 10% SDS-PAGE gel, agarose was used to overlayed the strip. The gel then was run at 40 mA/gel until the dyefront ran to the bottom of the gel. The gel was removed from the glass plate and placed in a glass plate with fixative solution (50% methanol, 12% acetic acid, and 0.05% formalin) shaking overnight.

Silver Staining

Silver staining was achieved using the Vorum silver staining method (first presented at the 48th American Society for Mass Spectrometry Conference on Mass Spectrometry June 11-15 2000, Long Beach, CA, poster TPE 191). The gel, submerged in fixative solution, was washed three times with 35% ethanol for twenty minutes each time shaking gently on a shaker. Following the Ethanol wash step, it is washed in ultrapure filtered deionized water for ten minutes each on a shaker. The gel then was sensitized with a solution consisting of 100 mM sodium thiosulfate (Fisher) and 30 mM potassium ferrocyanide (Amresco) for two minutes on a shaker. Then it was washed four times with ultrapure filtered deionized water for 10 minutes each on a shaker. Following the wash step, the gel was stained with 0.2% silver nitrate (Amresco) and 0.076% formalin (Protocol) for 20 minutes and then it was washed with ultrapure filtered deionized water twice for one minute each on a shaker. The gel was developed for 3-5 minutes using 6% sodium carbonate (VWR), 0.05% formalin, and 0.0004% sodium thiosulfate. Development of the gel was terminated using 50% Methanol and 12% acetic acid. Silver stained gels were scanned using a ScanMaker 9800XL (Microtek).

2-D Difference Gel Electrophoresis

Two-dimensional difference gel electrophoresis (2-D DIGE) was obtained from GE (Cat# RPK0272, RPK0273, RPK0275). The proteins of *N. fowleri* were solubilized in a lysis buffer and the protein concentration was determined as previously described. The lysis buffer mixture did not contain Tributyl phosphate (TBP). CyDye DIGE Fluors then were added to the protein lysate so that 50 ug of protein was labeled with 400 pmol of Fluor. The CyDyes and the protein of axenic and mouse passaged *N. fowleri* are paired in a following table fashion.

The protocol for the first dimension for 2-D DIGE is the same as previously described and the maximum volume of 300 uL of both protein mixture and the rehydration buffer was kept. Since the fluorescent properties of Cy2, Cy3 and Cy5 can be adversely affected by exposure to light, all labeling reactions were performed in the dark and light exposure was kept to a minimum.

The dry CyDyes were reconstituted in high quality anhydrous dimethylformamide (DMF) to yield a stock solution (2 nmol). From this stock solution, DMF is added to bring the final CyDye concentration to 400 pmoles/ul of the working CyDye concentration. Four-hundred pmol of CyDye per 40 ug of protein labeling is recommended. The second dimension of the gel electrophoresis was performed as described above. This phase of the separation procedure also was performed in the dark under minimum light exposure conditions.

Software

The 2-dimensional gels were analyzed using the software, PDQuest 2-D Analysis Software, purchased from Bio-Rad. The master-gel was created using triplicate gels and a scatter plot was generated using the replicated mater gel.

CyDye DIGE Fluors	Color (λ)	Amount
CyDye2	Yellow (488nm)	25ug of axenically-grown *N. fowleri* and 25ug of mouse-passaged *N. fowleri*
CyDye3	Red (532nm)	50 ug of axenically-grown *N. fowleri*
CyDye 5	Blue (635nm)	50ug of mouse-passaged *N. fowleri*

Table 2. Table of CyDye DIGE Fluors. This table represents CyDye DIGE Flours used in my research and its appropriate emitted color and its absorbed wavelength. CyDye2 was used as an internal control where equal amount of both strains of *N. fowleri* were added into a single reaction. CyDye3 was used to detect protein spots for axenically-grown *N. fowleri*, and CyDye 5 was used to detect protein spots for mouse-passaged *N. fowleri.*

.

Results

Culture of *N. fowleri*.

The mouse-passaged strain that has been linked to being highly pathogenic in mice, and the axenic strain that has been linked to being weakly pathogenic in mice, were generated as described previously (De Jonckheere, J. 1977). The three morphological stages that have been attributed to *N. fowleri* are shown in Figure 2. Before whole cell lysates of the ameboid form of either strain of *N. fowleri* was obtained, the amebae were screened for overt indication of bacterial contamination by scanning electron microscopy (SEM) (Figure 2). In addition, the culture medium from both strains was used for inoculation of Luria Broth Miller medium that was maintained in a 37°C incubator overnight in order to observe for signs of bacterial growth. These assessments were required since the axenic amebae were maintained on a bed of *E. coli*. No indication of bacterial contamination was seen following SEM or assessment of colony formation.

Infectivity of *N. fowleri* strains

To confirm that the mouse-passaged strain was highly pathogenic as compared with the axenic strain, a 50% infectious dose (i.e., ID_{50}) was determined. Amebae from each strain were counted using a hemocytometer and an equal concentration in an equal volume was used to inoculate mice (5/group) via the intranasal route. Infection of mice *with N. fowleri* was assessed based on stigmata that included a hunched-back, lack of movement, dehydration and loss of weight, and lack of response to tactile stimuli. In addition, infected mice demonstrated “raised” fur. Mice were sacrificed if they showed two or more of these typical symptoms. *N. fowleri*

passaged in mice exhibited a lower ID_{50} when compared to axenically-maintained amebae (Figure 3), consistent with the mouse-passaged amebae as being relatively more pathogenic.

Two-dimensional gel electrophoresis (2D-gel)

The protein expression profiles of the two strains of *N. fowleri* were analyzed following two-dimensional gel electrophoresis. Protein spots were analyzed over a pH range of 5-8 and a relative molecular weight (M_r) of 10 kiloDaltons (kD) – 160 kD. Thus, after focusing each protein spot was assigned an isoelectric point (pI):M_r coordinate value. Gels were performed in replicate to control for intra-experimental variation as well as for inter-experimental variation. To control for intra-experimental variation, replicate gels of protein profiles for axenically-grown amebae or mouse-passaged amebae were used to create master gels (Study A) that were representative of axenically-grown amebae or mouse-passaged amebae, respectively. To control for inter-experimental variation, this previous protocol for creation of master gels was repeated (Study B) using a separate lot of axenically-grown or mouse-passaged amebae. Three gels were analyzed in Study A and two gels were analyzed in Study B. Representative gels for axenically-grown amebae are shown in Figures 4 and 6 while those for mouse-passaged amebae are shown in Figures 5 and 7. Gaussian representations of differentially expressed spots for axenically-grown amebae and for mouse-passaged amebae are shown in Figures 8 and 9. The protein profile fingerprint for axenically–grown amebae versus mouse-passaged amebae was distinctive. In addition, a greater number of protein spots was present in the protein profile for axenically-maintained amebae.

Two representative gels from Study A were used to create a Scatter Plot for axenically-grown *N. fowleri* (Figure 10). The spots depicted in the scatter plot are present in both gels and

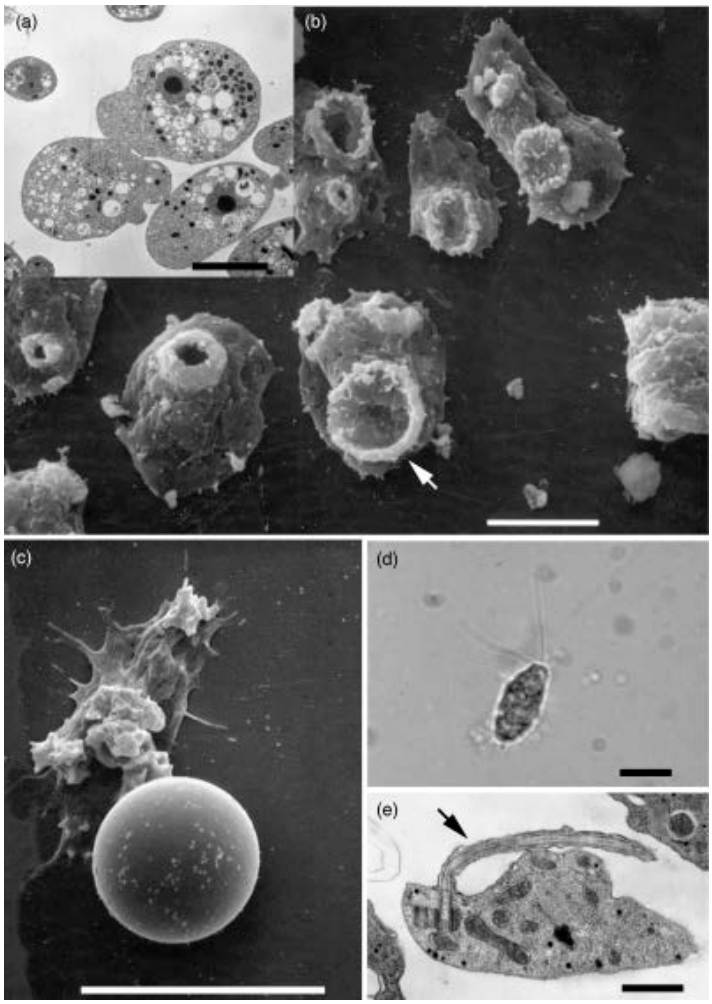

Figure 2. Scanning electron micrographs of the three morphological stages of *Naegleria fowleri.*

(a) Transmission electron micrograph (TEM) of trophozoites illustrating the prominent nucleus with a centrally located electron-dense nucleolus. (b) Scanning electron micrograph (SEM) of trophozoites exhibiting 'food-cups' (arrow). (c) SEM of a cyst. (d) Light micrograph of a flagellate with the characteristic two flagella. (e) TEM of flagellate illustrating one of the flagella (arrow). The scale bars represent 10 μm for (a–d) and 2 μm for (e). Typical *N. fowleri* stages include a dormant cyst, a feeding trophozoite, and a transient swimming flagellate. Image adapted from: Marciano-Cabral, F., and G. Cabral., 2007. The Immune response to *Naegleria fowleri* amebae and pathogenesis of infection. FEMS Immunol. Med. Microbiol. 51:243-259.

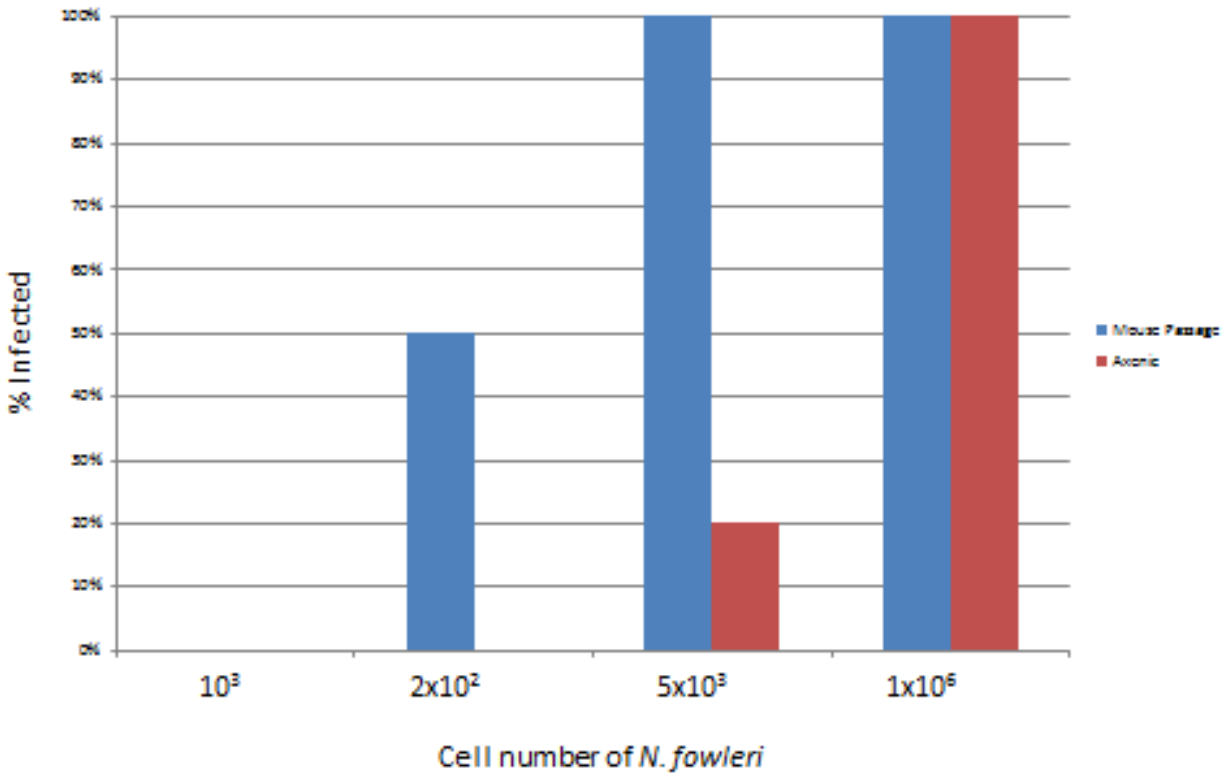

Figure 3. Infectious dose of mouse-passaged *N. fowleri* versus axenically-passaged N. *fowleri*. The *N. fowleri* were counted using a hemocytometer and inoculated into the muse nasal cavity and observed for 7 days for symptoms of infection. The ID_{50} for the mouse-passaged strain was 200 while that for the axenically-grown strain was 11,857. When observed, mice were humanely euthanized (data obtained from Dr. Francine Marciano-Cabral).

the density level is plotted along both axes. A correlation coefficient (R-value) of 0.90 was obtained. The green line on the scatter plot represents the best fit line. The blue line above the green line represents the best fit line for two standard deviations of differential levels of protein designated on the ordinate axis (i.e., y-axis). The red line below the green line represents the best fit line for two standard deviations of differential level of protein designated on the abscissa axis (i.e., x-axis). Similarly, using replicate gels from Study B, a Scatter Plot was generated for the axenically-grown *N. fowleri* (Figure 11). Finally, the master gels from Study A and Study B representing axenically-grown *N. fowleri* were compared for correlation (Figure 12).

A similar process was employed for comparison of gels from mouse-passaged *N. fowleri*. The scatter plots of 2-D gels from Study A and Study B for mouse- passaged *N. fowleri* are shown in Figures 13 and 14. A correlation coefficient of 0.93 was observed for Study A and 0.90 was observed for Study B. The master gels of mouse- passaged *N. fowleri* whole cell lysates for Study A and Study B were plotted against each other and a correlation coefficient of 0.90 was observed (Figure 15).

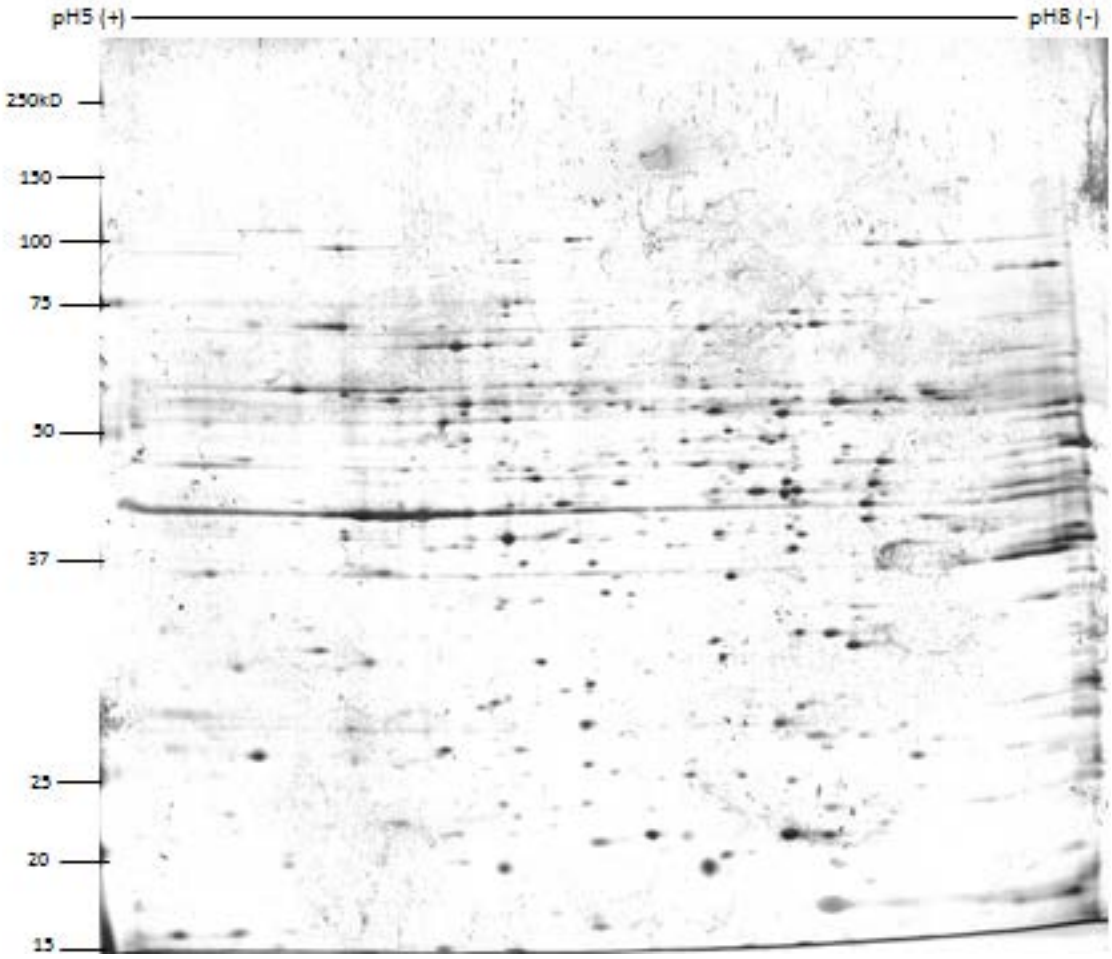

Figure 4. Representative two-dimensional electrophoresis gel of axenically-grown *N. fowleri* (Study A). The whole cell lysate (50 ug) was separated in the first dimension over a pH range of 5 to 8 and in the second dimension on 10% SDS-PAGE. The two-dimensional gel was stained using a Vorum silver staining method as previously described (Vorum, H. 2004). The numbers on the left margin designate relative molecular weights in kiloDaltons (kD). The label on the top of the gel designates the pH range for first dimension isoelectric focusing.

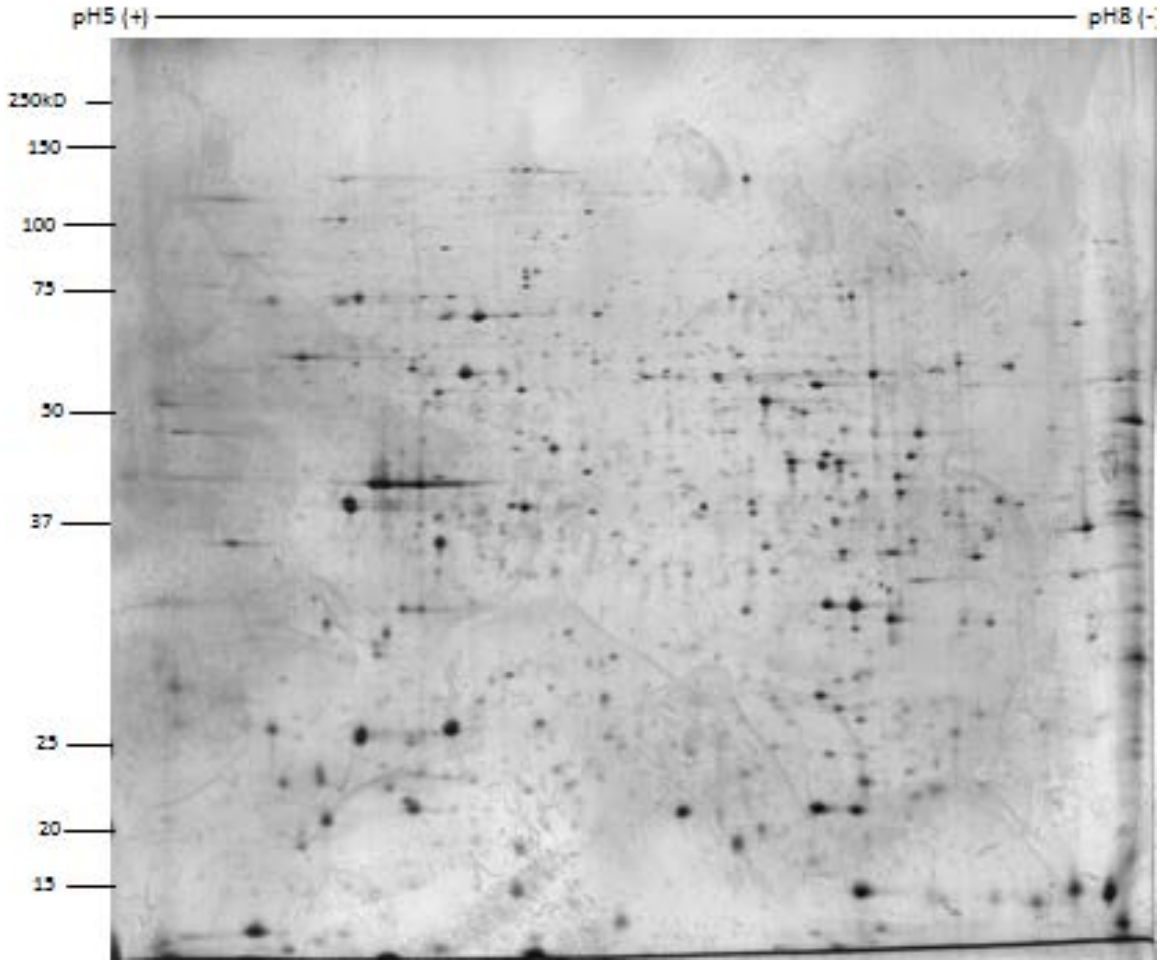

Figure 5. Representative two-dimensional electrophoresis gel of mouse-passaged *N. fowleri* (Study A). The whole cell lysate (50 ug) was separated in the first dimension over a pH range of 5 to 8 and in the second dimension on 10% SDS-PAGE. The two-dimensional gel was stained using a Vorum silver staining method as previously described (Vorum, H. 2004). The numbers on the left margin designate relative molecular weights in kiloDaltons (kD). The label on the top of the gel designates the pH range for first dimension isoelectric focusing.

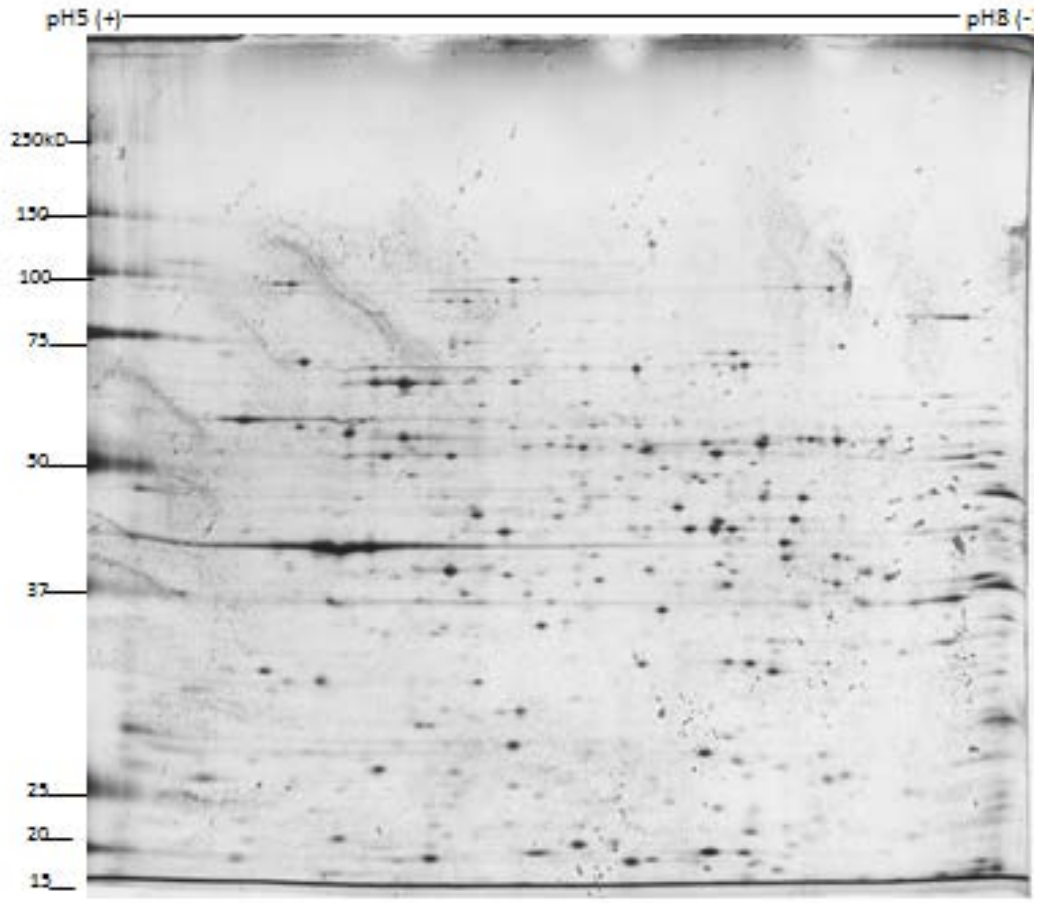

Figure 6. Replicated study (Study B) of two-dimensional electrophoresis gel of axenically-grown *N. fowleri*. The whole cell lysate (50 ug) was separated in the first dimension over a pH range of 5 to 8 and in the second dimension on 10% SDS-PAGE. The two-dimensional gel was stained using a Vorum silver staining method as previously described (Vorum, H. 2004). The numbers on the left margin designate relative molecular weights in kiloDaltons (kD). The label on the top of the gel designates the pH range for first dimension isoelectric focusing.

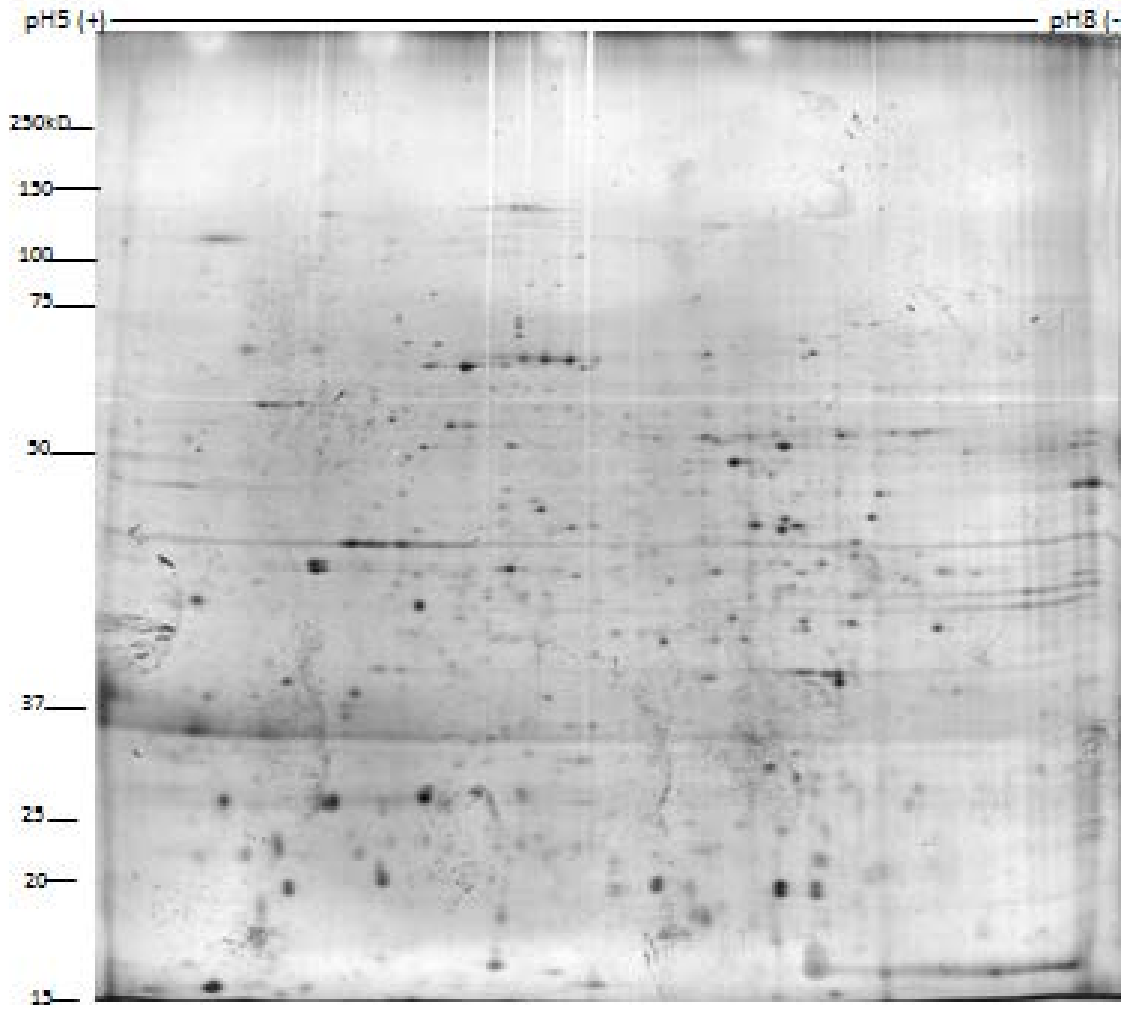

Figure 7. Replicated Study (Study B) of two-dimensional electrophoresis gel of mouse-passaged *N. fowleri*. The whole cell lysate (50 ug) was separated in the first dimension over a pH range of 5 to 8 and in the second dimension on 10% SDS-PAGE. The two-dimensional gel was stained using a Vorum silver staining method as previously described (Vorum, H. 2004). The numbers on the left margin designate relative molecular weights in kiloDaltons (kD). The label on the top of the gel designates the pH range for first dimension isoelectric focusing.

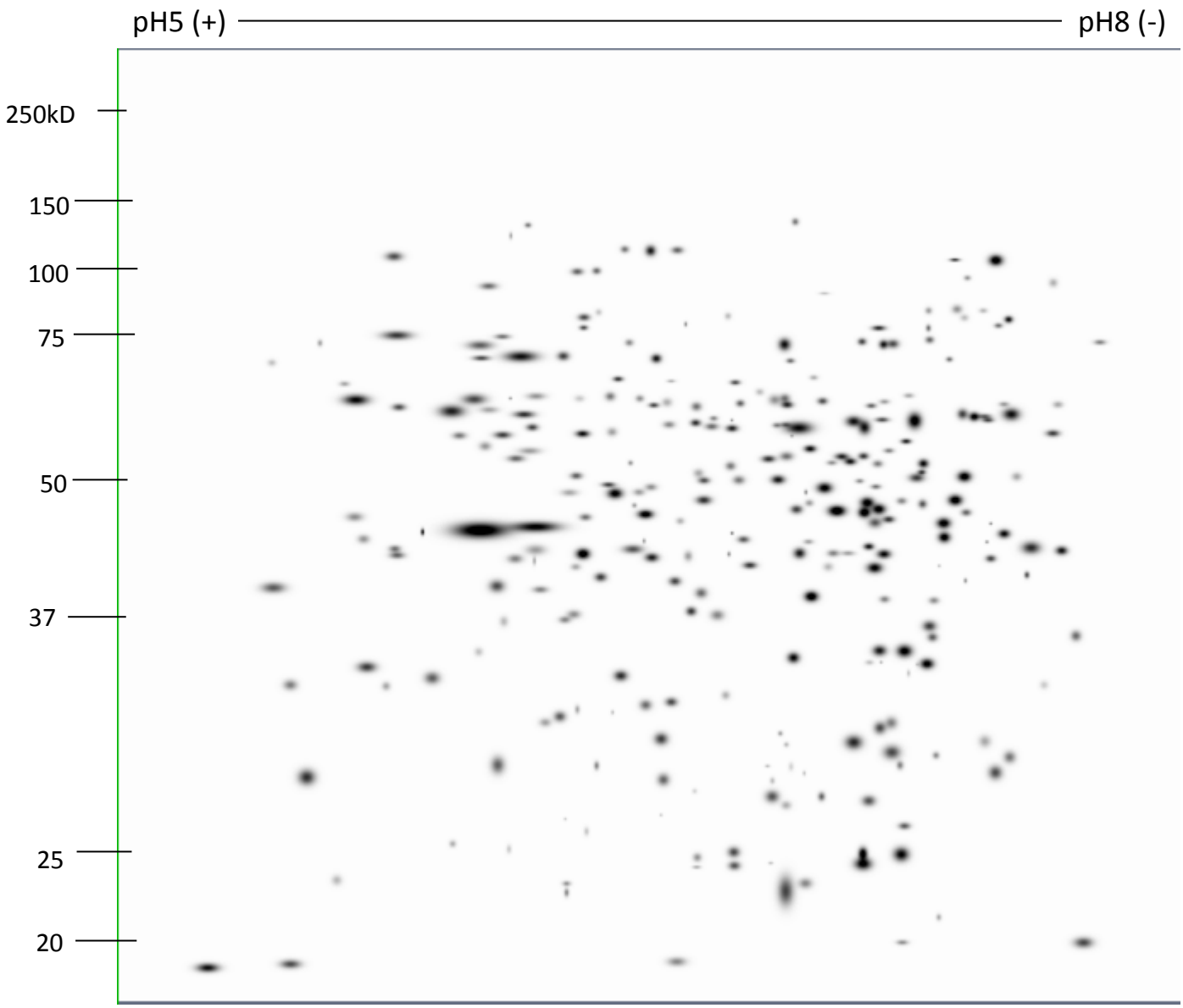

Figure 8. Gaussian image of master gel of axenically-grown *N. fowleri*. The master gel was created from three replicated 2-D electrophoresis gels. This master gel template was used as a reference map that summarizes the protein levels observed from the three replicated gels. Each spot represents a Gaussian image of the representative protein spot and was assigned a pI:M_r coordinate value.The numbers at the left margin designate relative molecular weights in kiloDaltons (kD). The label at the top of the gel designates the pH range for first dimension isoelectric focusing.

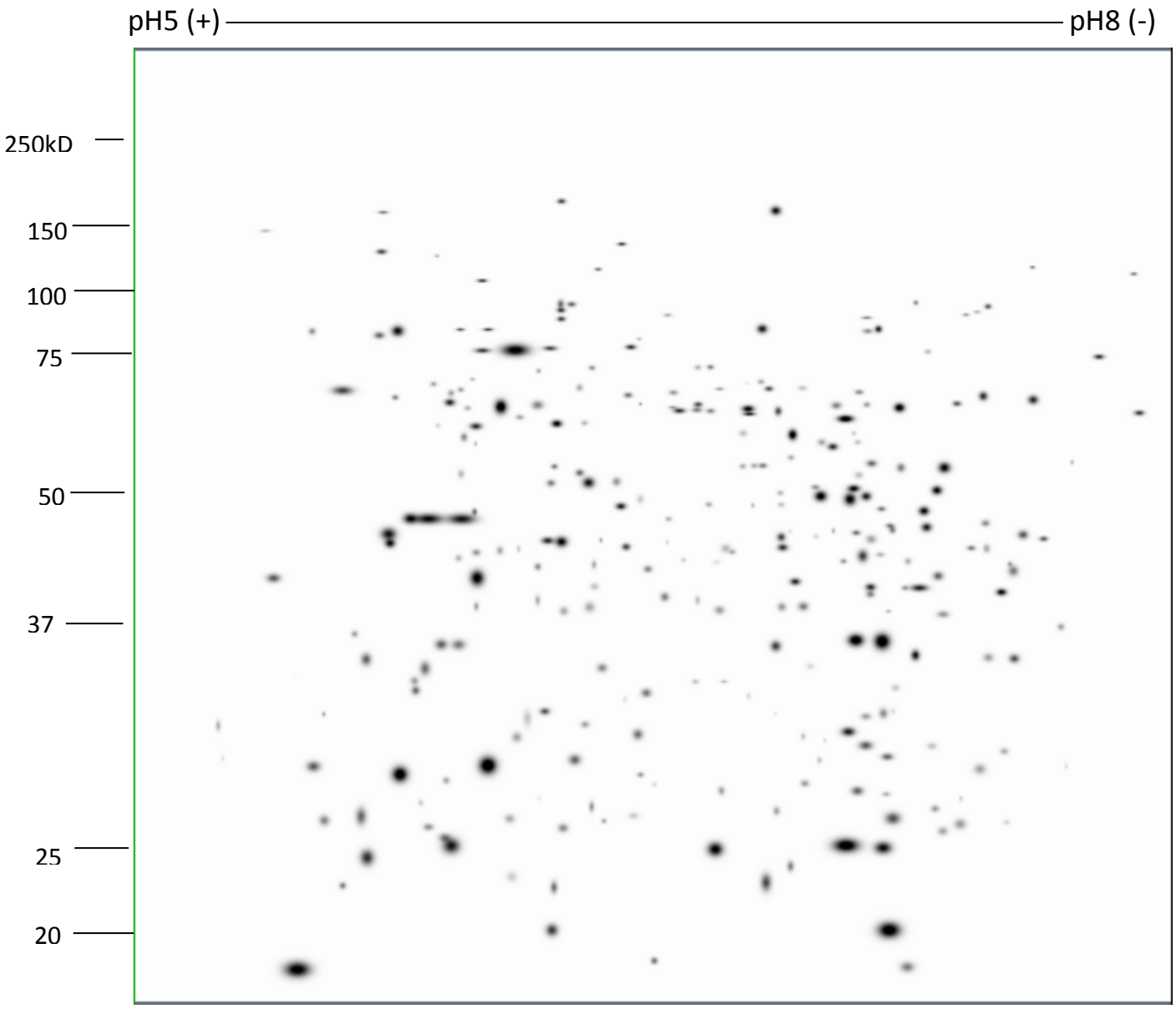

Figure 9. Gaussian image of master gel of mouse-passaged *N. fowleri*. The master gel was created from the three replicated 2-D electrophoresis gels. This master gel template was used as a reference map that summarizes the protein levels observed from three replicated gels. Each spot represents a Gaussian image of the representative protein spot and was assigned a pI:M_r coordinate value.. The numbers at the left margin designate relative molecular weights in kiloDaltons (kD). The label at the top of the gel designates the pH range for first dimension isoelectric focusing.

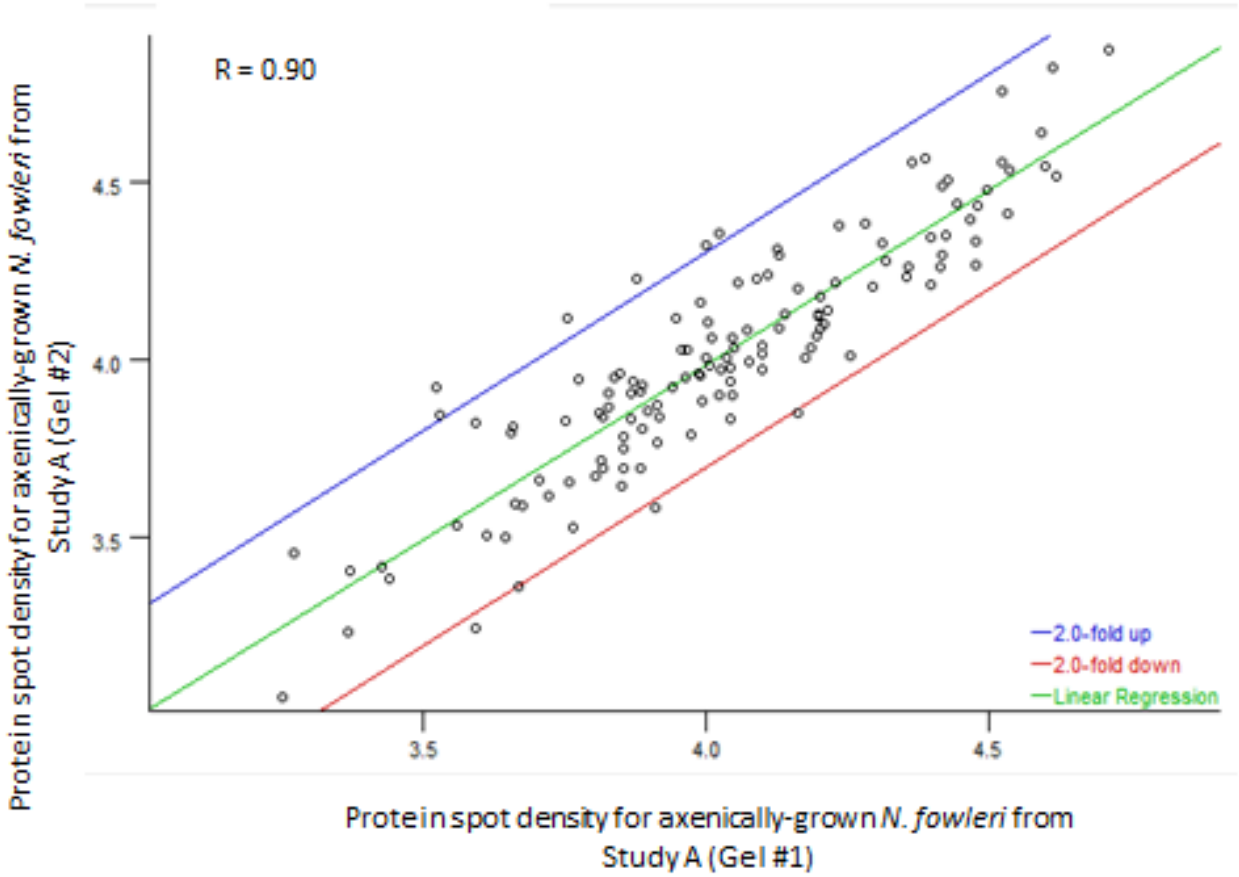

Figure 10. Scatter plot generated using two representative gels of axenically-grown *N. fowleri* in Study A. Individual dots represent protein spots present in replicate gels for axenically-grown *N. fowleri*. The green line on each scatter plot represents the best fit line. The blue line above the green line represents the best fit line for two standard deviations of differential level of protein designated on the ordinate axis (i.e., y-axis). The red line below the green line represents the best fit line for two standard deviations of differential level of protein designated on the abscissa axis (i.e., x-axis).

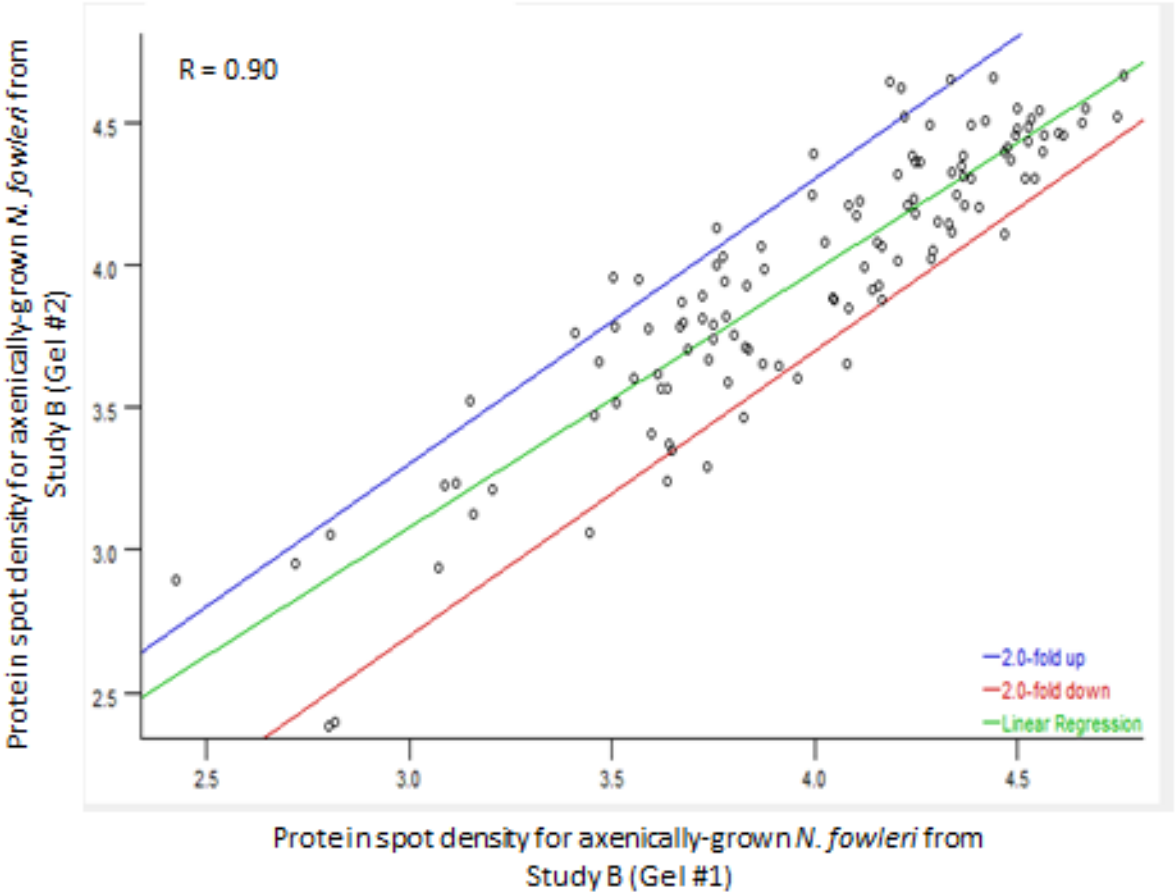

Figure 11. Scatter plot generated using two representative gels of axenically-grown *N. fowleri* in Study B. Individual dots represent protein spots present in replicate gels for axenically-grown *N. fowleri*. The green line on each scatter plot represents the best fit line. The blue line above the green line represents the best fit line for two standard deviations of differential level of protein designated on the ordinate axis (i.e., y-axis). The red line below the green line represents the best fit line for two standard deviations of differential level of protein designated on the abscissa axis (i.e., x-axis).

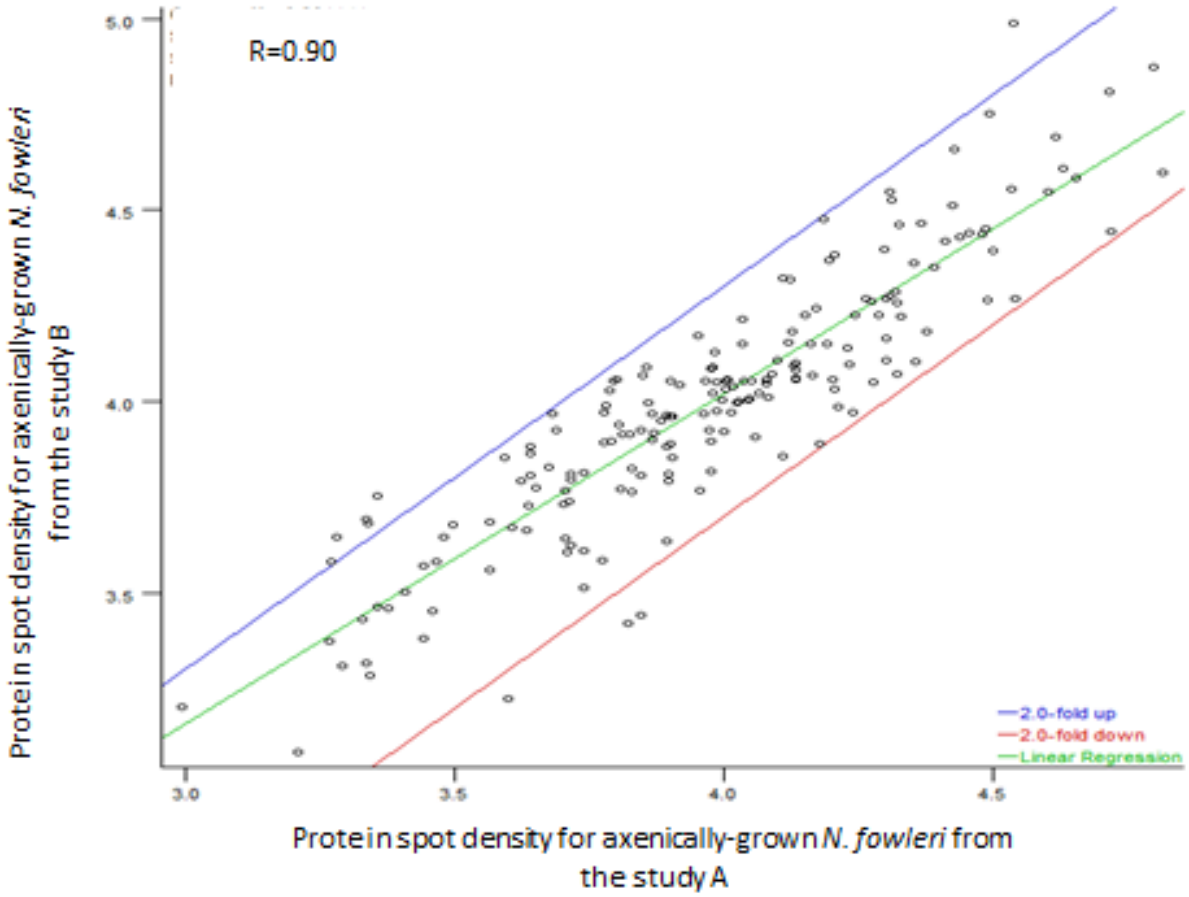

Figure 12. Scatter plot generated using the two-dimensional electrophoresis gels from axenically-grown *N. fowleri* from study A versus axenically-grown *N. fowleri* from study B. Individual dots represent protein spots present in master gels for axenically-grown *N. fowleri*. The green line on each scatter plot represents the best fit line. The blue line above the green line represents the best fit line for two standard deviations of differential level of protein designated on the ordinate axis (i.e., y-axis). The red line below the green line represents the best fit line for two standard deviations of differential level of protein designated on the abscissa axis (i.e., x-axis).

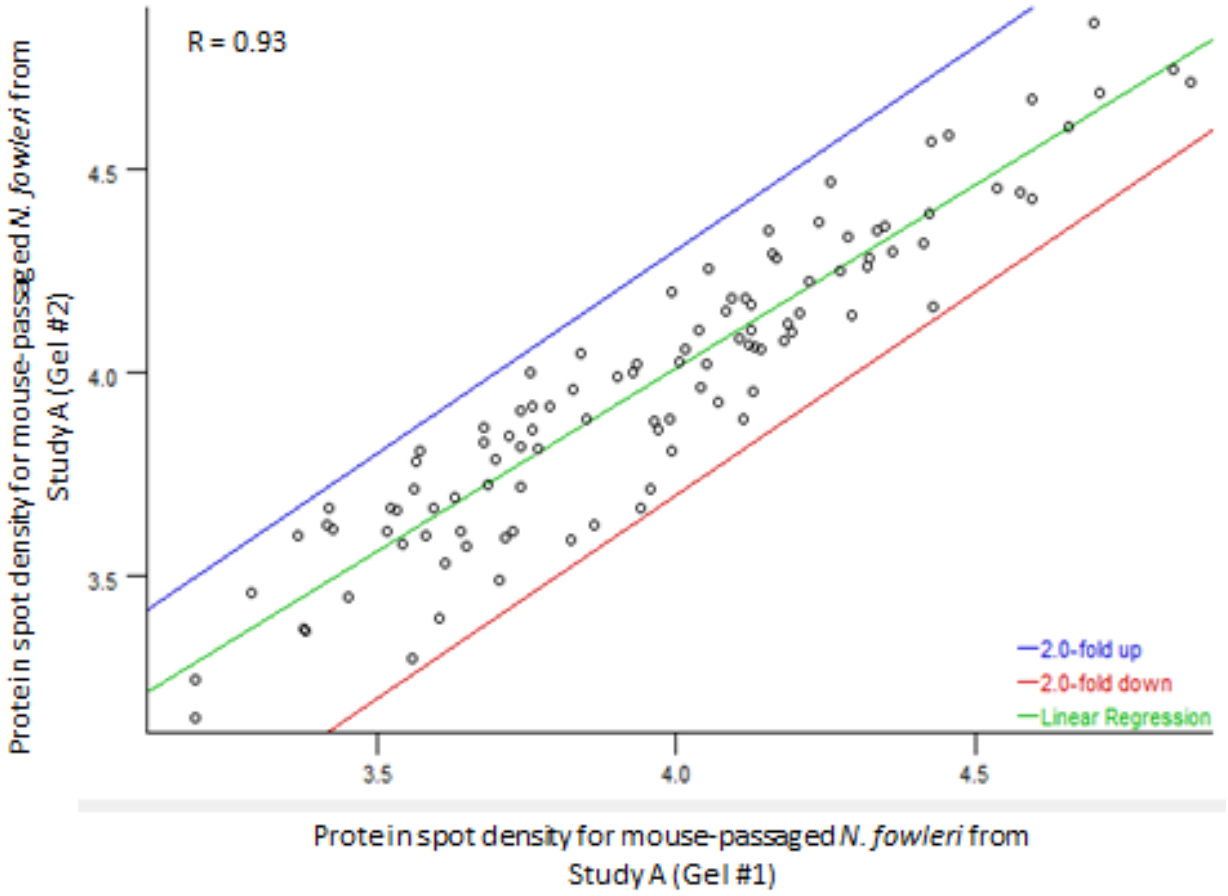

Figure 13. Scatter plot generated using two representative gels of mouse-passaged *N. fowleri* in Study A. Individual dots represent protein spots present in replicate gels for mouse-passaged *N. fowleri*. The green line on each scatter plot represents the best fit line. The blue line above the green line represents the best fit line for two standard deviations of differential level of protein designated on the ordinate axis (i.e., y-axis). The red line below the green line represents the best fit line for two standard deviations of differential level of protein designated on the abscissa axis (i.e., x-axis).

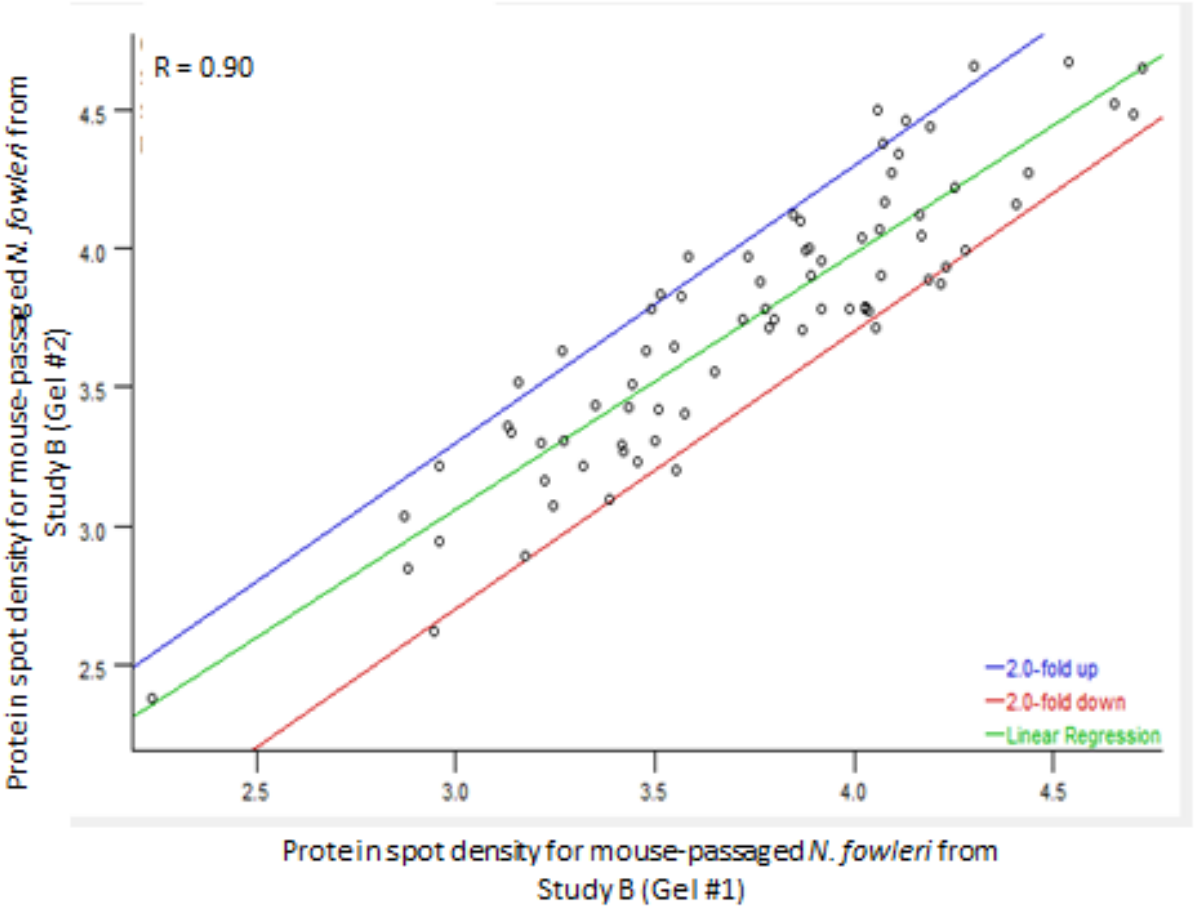

Figure 14. Scatter plot generated using two representative gels of mouse-passaged *N. fowleri* in Study B. Individual dots represent protein spots present in replicate gels for mouse-passaged *N. fowleri*. The green line on each scatter plot represents the best fit line. The blue line above the green line represents the best fit line for two standard deviations of differential level of protein designated on the ordinate axis (i.e., y-axis). The red line below the green line represents the best fit line for two standard deviations of differential level of protein designated on the abscissa axis (i.e., x-axis).

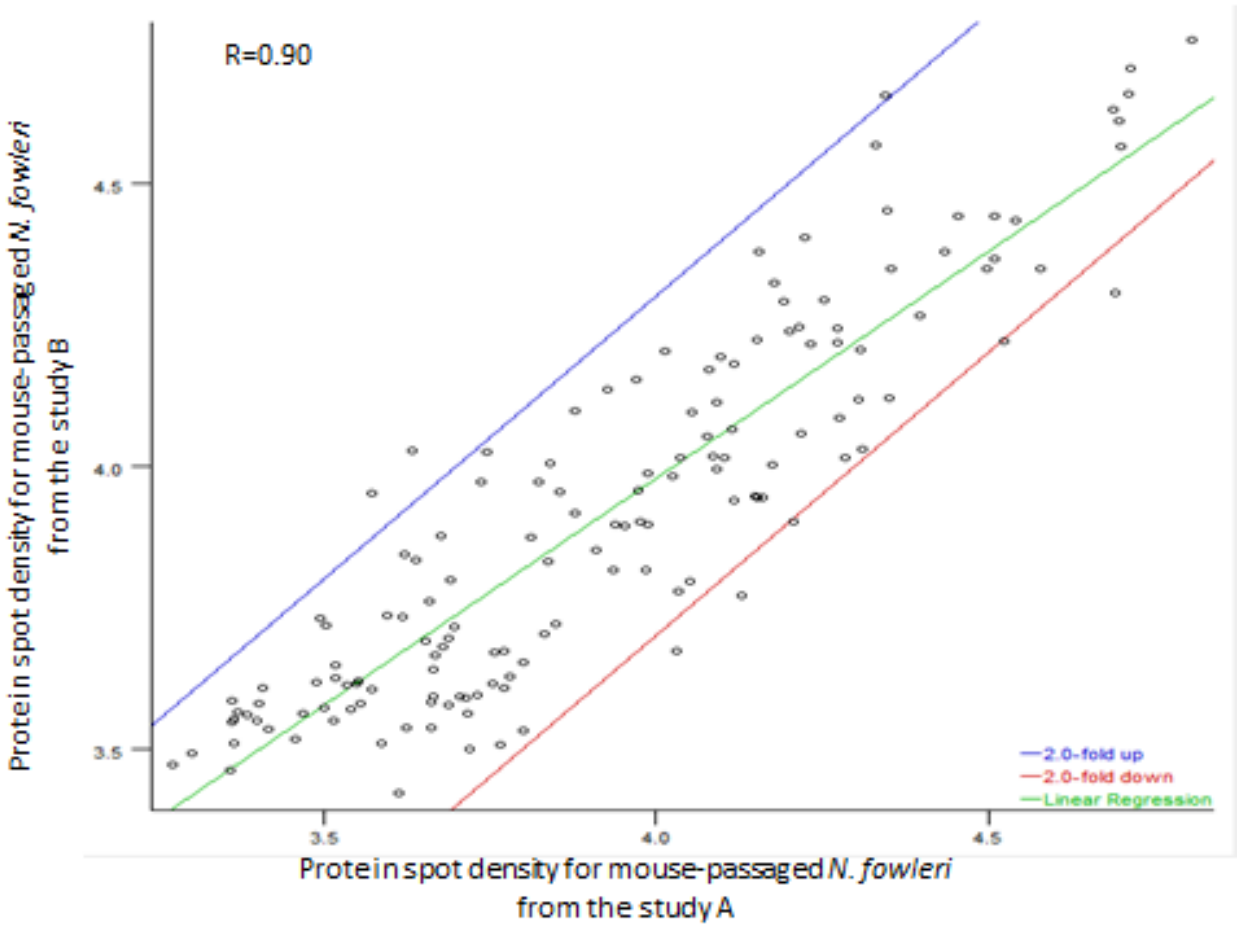

Figure 15. Scatter plot generated using the two-dimensional electrophoresis gels from mouse-passaged *N. fowleri* from study A mouse-passaged *N. fowleri* from study B. Individual dots represent protein spots represent master gels for mouse-passaged *N. fowleri*. The green line on each scatter plot represents the best fit line. The blue line above the green line represents the best fit line for two standard deviations of differential level of protein designated on the ordinate axis (i.e., y-axis). The red line below the green line represents the best fit line for two standard deviations of differential level of protein designated on the abscissa axis (i.e., x-axis).

Two-Dimensional Difference Gel Electrophoresis (2-D DIGE)

The Vorum silver staining used for visualizing protein spots on two-dimensional gels indicated that axenally-grown and mouse-passaged *N. fowleri* had different protein signature profiles. In order to confirm these results, two-dimensional difference gel electrophoresis was performed. The use of different cyanine fluorescent dyes and a mixed internal standard allowed for direct comparison of protein profiles attributed to axenically-grown versus mouse-passaged *N. fowleri*. DIGE confirmed that both strains of *N. fowleri* presented a differential proteomic profile. Three-dimensional imaging indicated that some spots representative of proteins were elevated in mouse-passaged amebae when compared to the axenically-grown amebae. Conversely, some spots representative of proteins were decreased in level in mouse-passaged amebae when compare to the axenically-grown amebae (Figure 16).

Comparative proteomic analysis of axenically-grown and mouse-passaged *N. fowleri*

Figure 17 depicts a scatter plot of measured density of protein spots from master gels of axenically-grown and mouse-passaged *N. fowleri*. Two-dimensional electrophoresis gels from Study A were chosen as a representative group for analysis because between Study A and B the correlation value of 0.90 was observed for both axenically-grown and mouse-passaged amebae and Study A has higher number of gels that can be analyzed. As shown from the scatter plot, the protein spots below the red line indicate a subset of proteins that are expressed at higher levels or preferentially in axenically-grown of *N. fowleri*. The spots indicative of proteins localized above the blue line indicate a subset of proteins that are expressed at higher levels or preferentially in mouse-passaged *N. fowleri*. A correlation coefficient of 0.60 was observed when 2-D gels for axenically-grown versus mouse-passaged amebae were plotted, consistent with the presence of a

distinctive proteomic fingerprint indicative of an axenically-grown state versus that of a mouse-passaged state.

Protein spots of interest

Using the scatter plot graphs and "Spot Review" function in PDQuest as a tool, a representative subset of proteins was selected for further analysis. Further analysis included three dimensional viewing as well as interpretation of the density of the respective protein spot between gels using a bar graph. The protein numbers were randomly assigned by the PDQuest software (Figures 18 to 33). The Cartesian coordinates were generated using the representative two-dimensional electrophoresis gels for mouse-passaged and axenically-grown *N. fowleri* (Table 2).

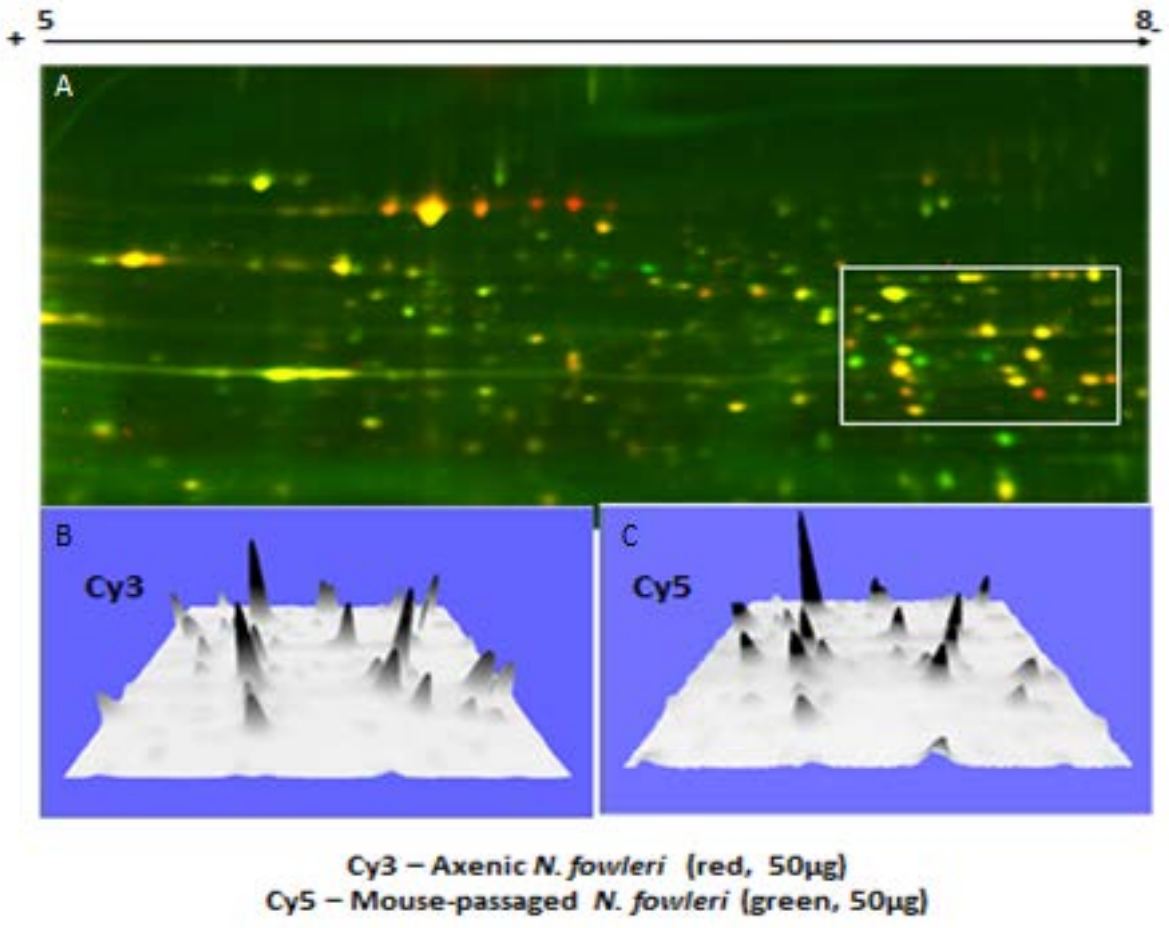

Figure 16. Two-dimensional fluorescence difference gel electrophoresis (2-D DIGE) of axenically-grown *N. fowleri* and mouse-passaged *N. fowleri*. Panel A: Two-dimensional Fluorescence difference gel electrophoresis profile. The label at the top of the gel designates the pH range for first dimension isoelectric focusing. The sample was run in the second dimension on a 10% SDS-polyacrylamide gel. Spots indicated in "green" represent proteins that are expressed in the mouse-passaged amebae. Spots indicated in "red" represent proteins that are expressed in axenically-grown amebae. Spots indicated in "yellow" represent proteins that are expressed in common and at approximately equal levels in both mouse-passaged and axenically-grown amebae. Spots indicated in "orange" represent proteins that are differentially expressed in axenically-grown versus mouse-passaged amebae. (Figure courtesy of Dr. Melissa Jamerson). Panels B and C are three-dimensional representations of the differential protein expression indicated in the boxed area shown in Panel A.

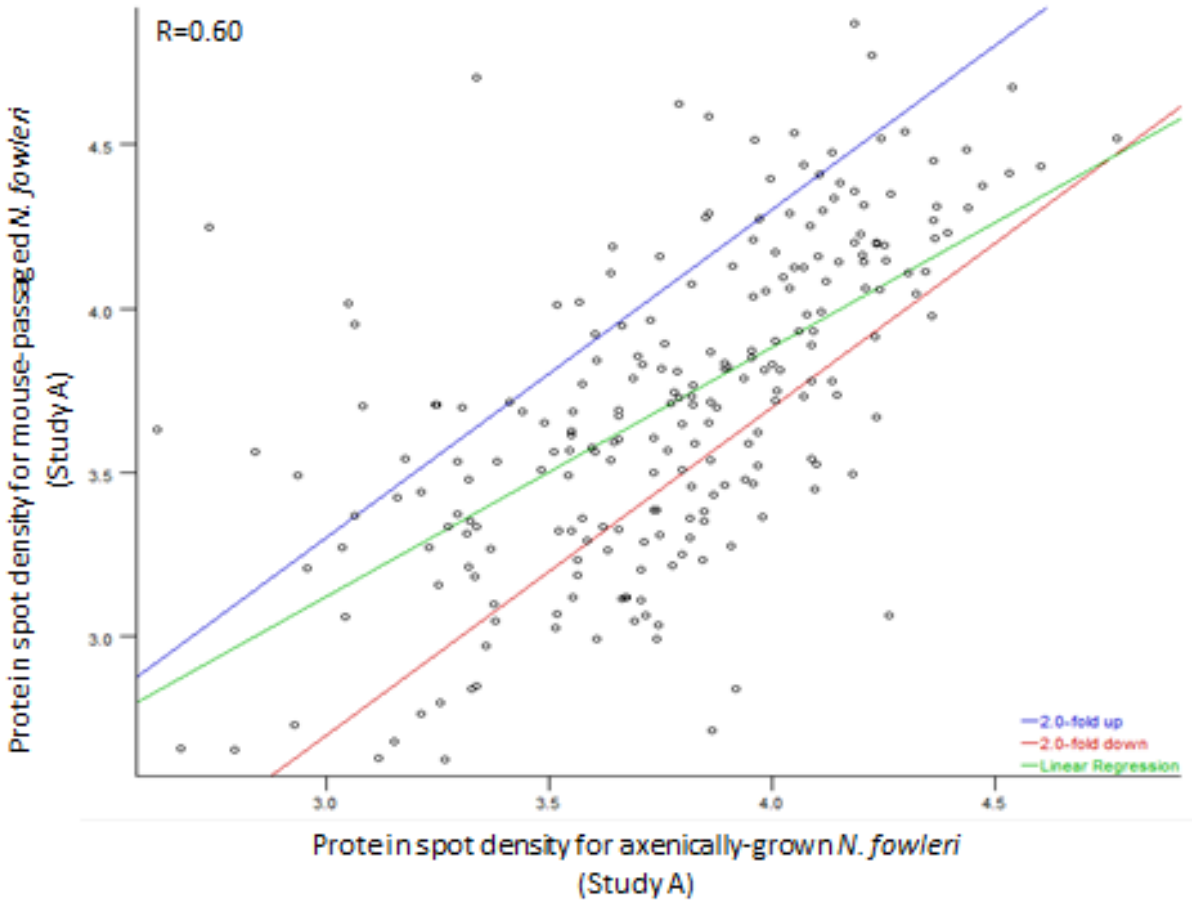

Figure 17. Scatter plot generated using the master two-dimensional electrophoresis gels from axenically-grown *N. fowleri* versus mouse-passaged *N. fowleri* (Study A). The green line on each scatter plot represents the best fit line. The blue line above the green line represents the best fit line for two standard deviations of differential higher level of protein as designated on the ordinate axis (i.e., y-axis) for mouse-passaged *N. fowleri*. The red line below the green line represents the best fit line for two standard deviations higher level of protein as designated on the abscissa axis (i.e., x-axis) for axenically-grown *N. fowleri*.

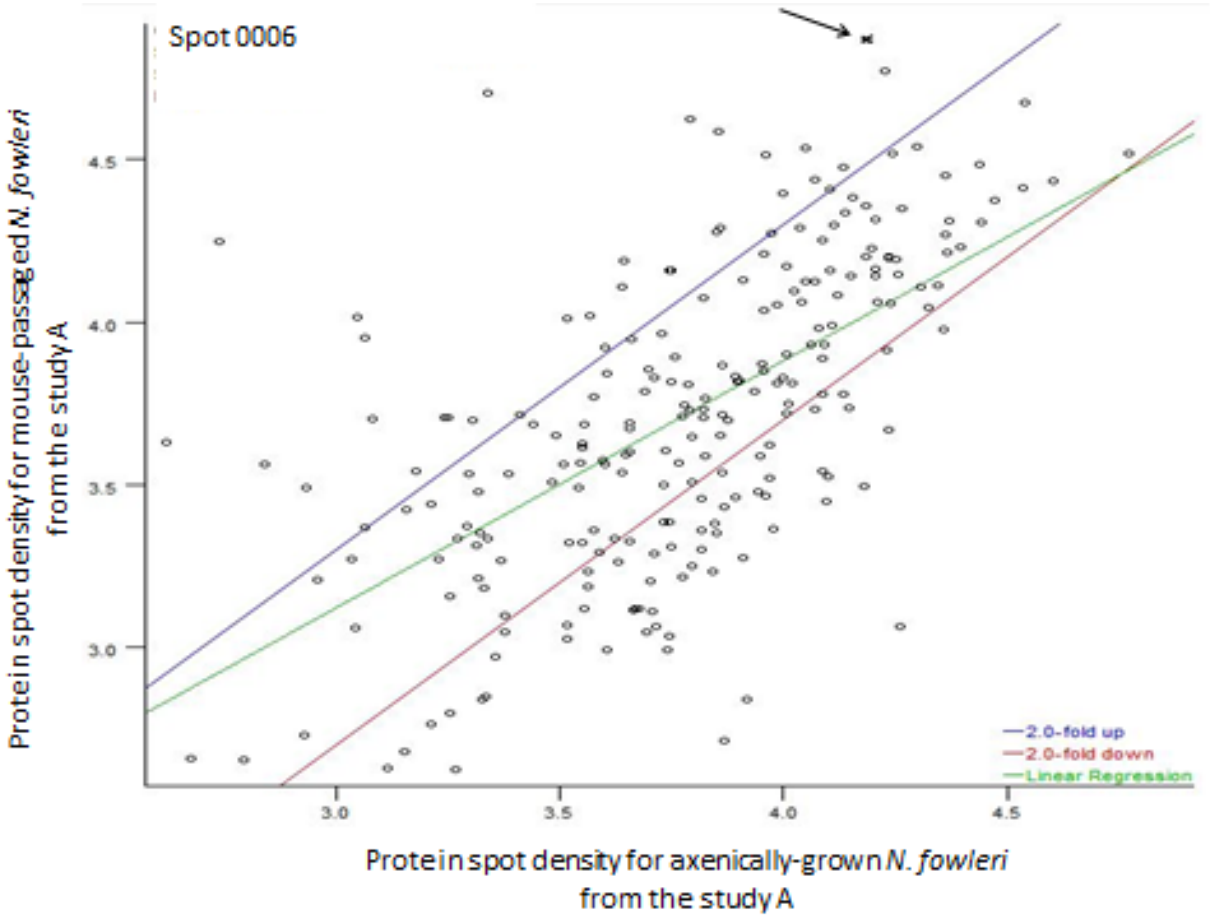

Figure 18. Scatter plot location of Spot 0006. The arrow indicates the location of the protein in a density scatter plot for mouse-passaged versus axenically-grown *N. fowleri*.

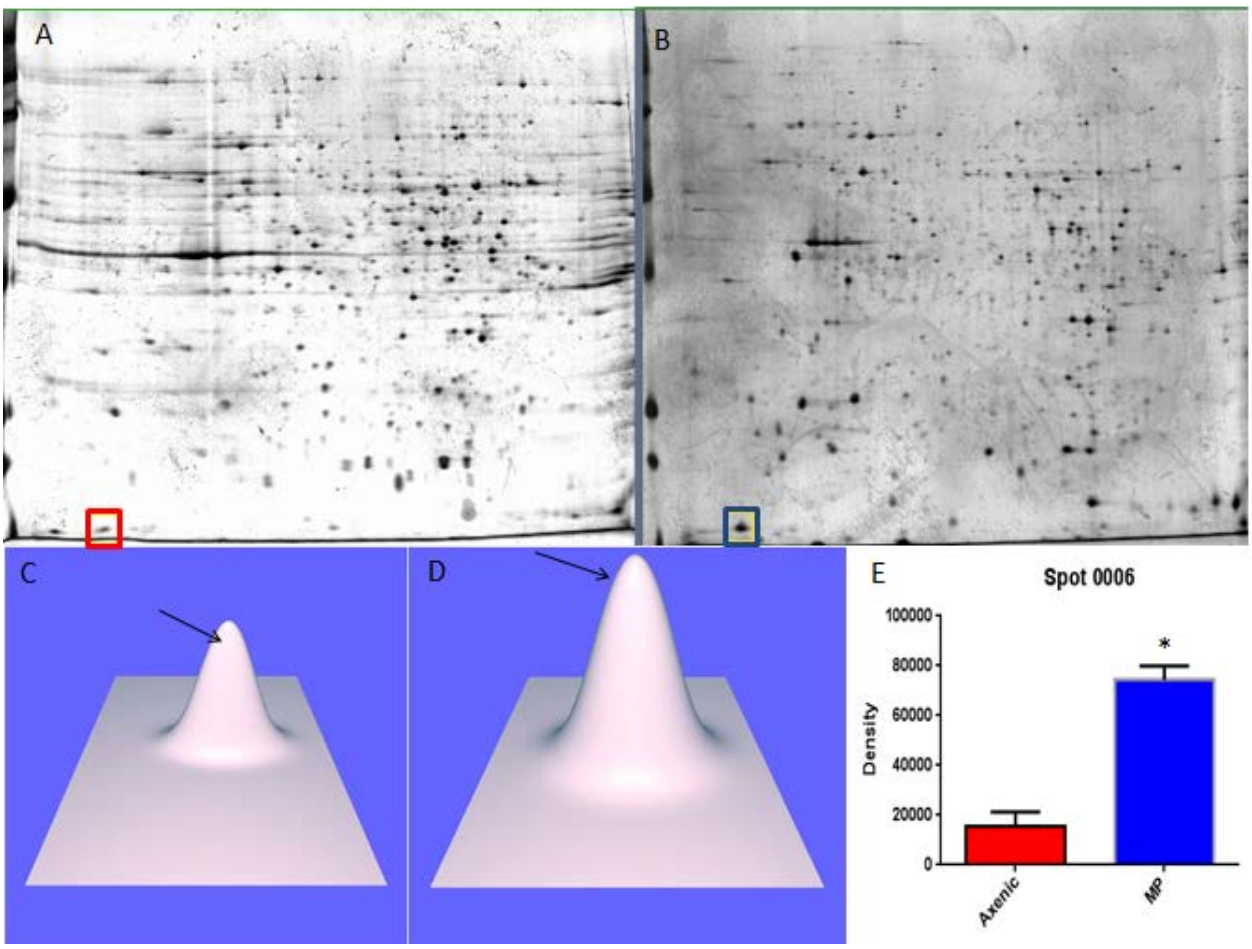

Figure 19. Analysis of spot 0006. The red box in Panel A and the blue box in Panel B show the location of the protein spot on two dimensional electrophoresis gels for axenically-grown (A) and mouse-passaged (B) *N. fowleri*, respectively. Panels C and D represent the three dimensional rendering of the level of protein that is observed. Panel E is represented in a bar graph fashion and demonstrates the reproducibility of spot detection for each of the three gels that served as a composite for the master gel. Note that the density level of protein for the given spot is elevated for the mouse-passaged three-dimensional image compared to the axenic counterpart. An analysis of the density values by Student's t-test indicates a p-value of 0.0002. Since this is below our significance level of 0.05, we can conclude that the density values have a statistically significant difference indicated by an asterisk (*).

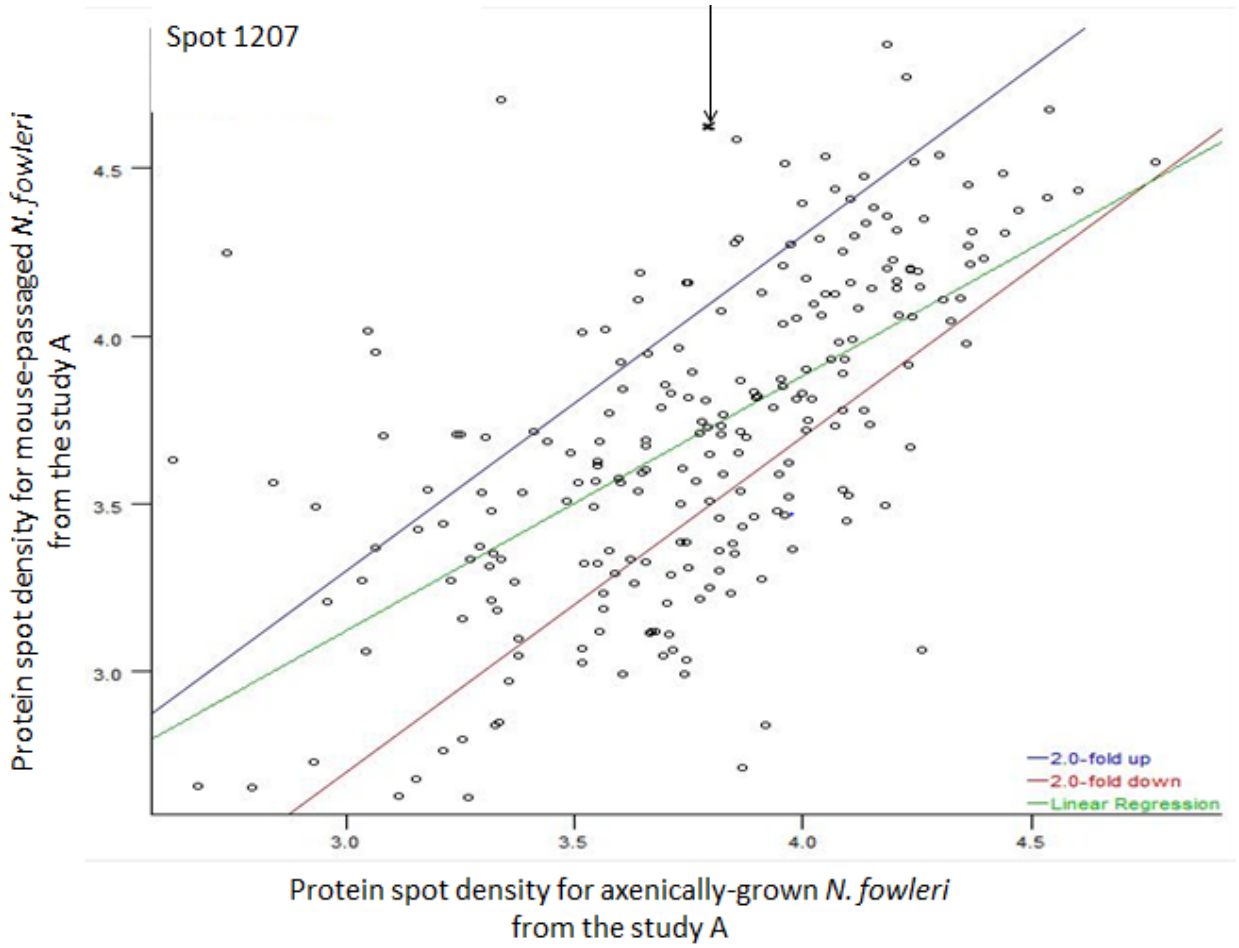

Figure 20. Scatter plot location of spot 1207. The arrow indicates the location of the protein in a density scatter plot for mouse-passaged versus axenically-grown *N. fowleri*.

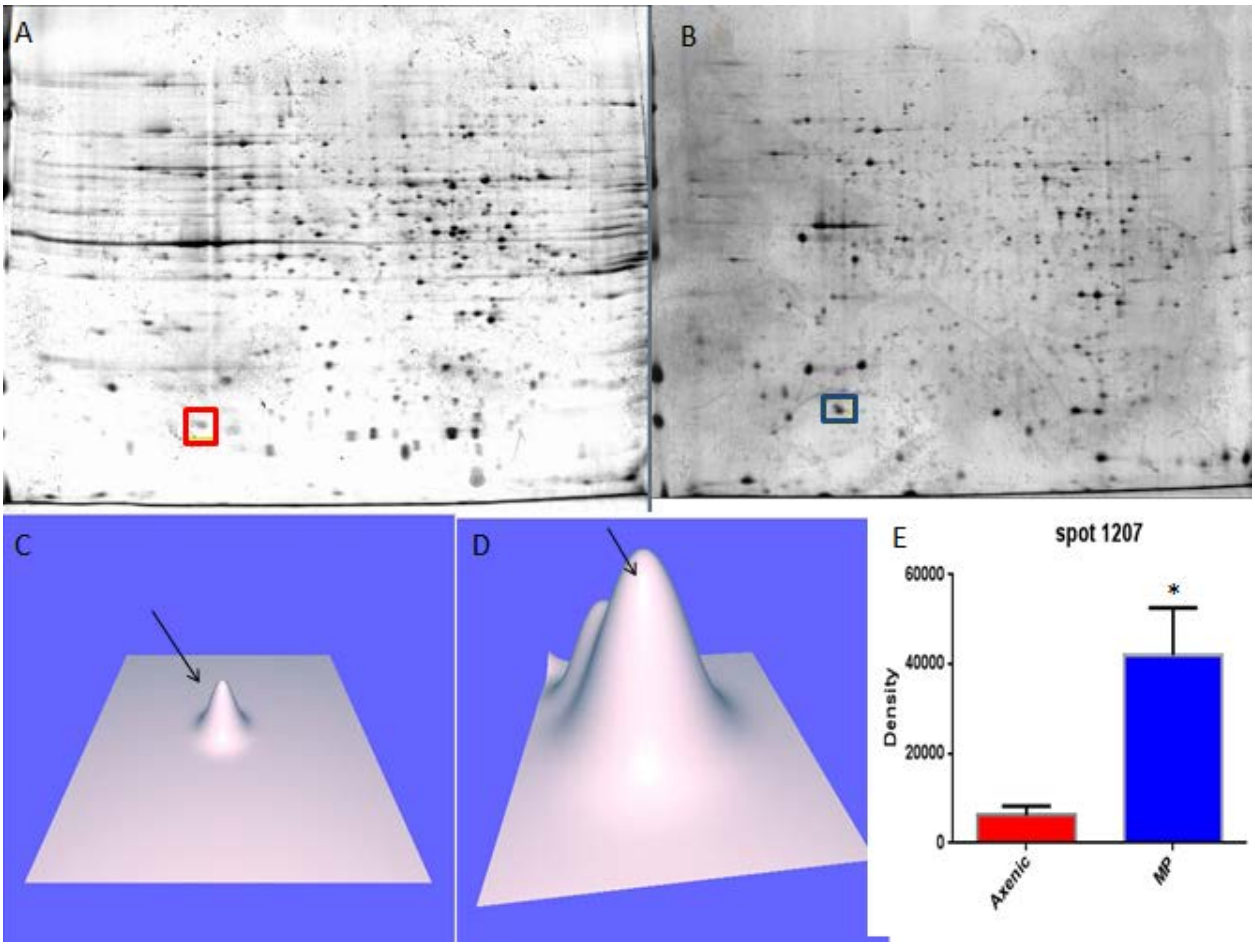

Figure 21. Analysis of spot 1207. The red box in Panel A and the blue box in Panel B show the location of the protein spot on two dimensional electrophoresis gels for axenically-grown (A) and mouse- passaged (B) *N. fowleri*, respectively. Panels C and D represent the three-dimensional rendering of the level of protein that is observed. Figure E is represented in a bar graph fashion and demonstrates the reproducibility of spot detection for each of the three gels that served as a composite for the master gel. Note that the density level of protein for the given spot is elevated for the mouse-passaged three-dimensional image compared to the axenically-grown counterpart. A bimodal peak is present in Panel D. An analysis of the density values by Student's t-test indicates a p-value of 0.0047. Since this is below our significance level of 0.05, we can conclude that the density values have a statistically significant difference indicated by an asterisk (*).

.

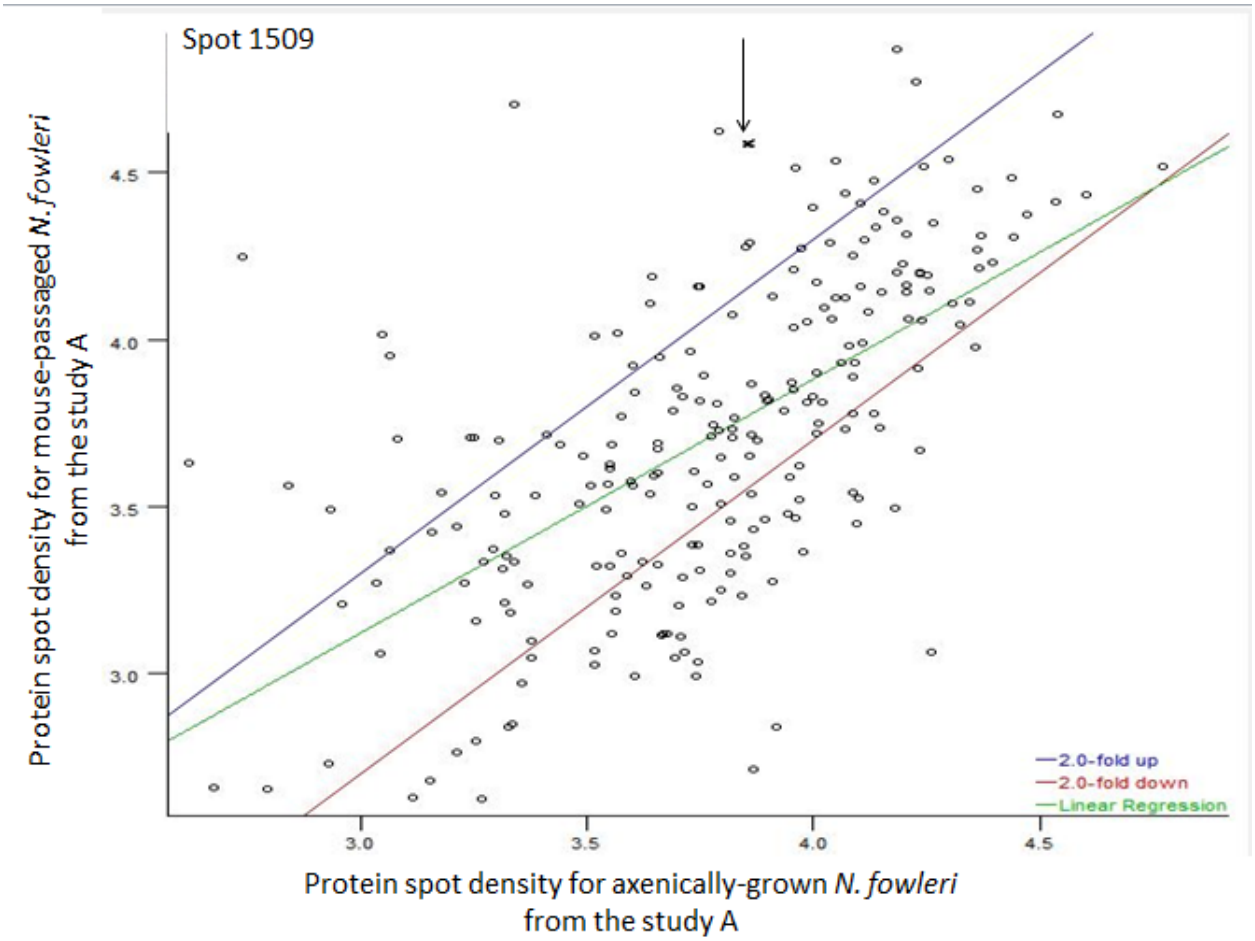

Figure 22. Scatter plot location of spot 1509. The arrow indicates the location of the protein in a density scatter plot for mouse-passaged versus axenically-grown *N. fowleri*.

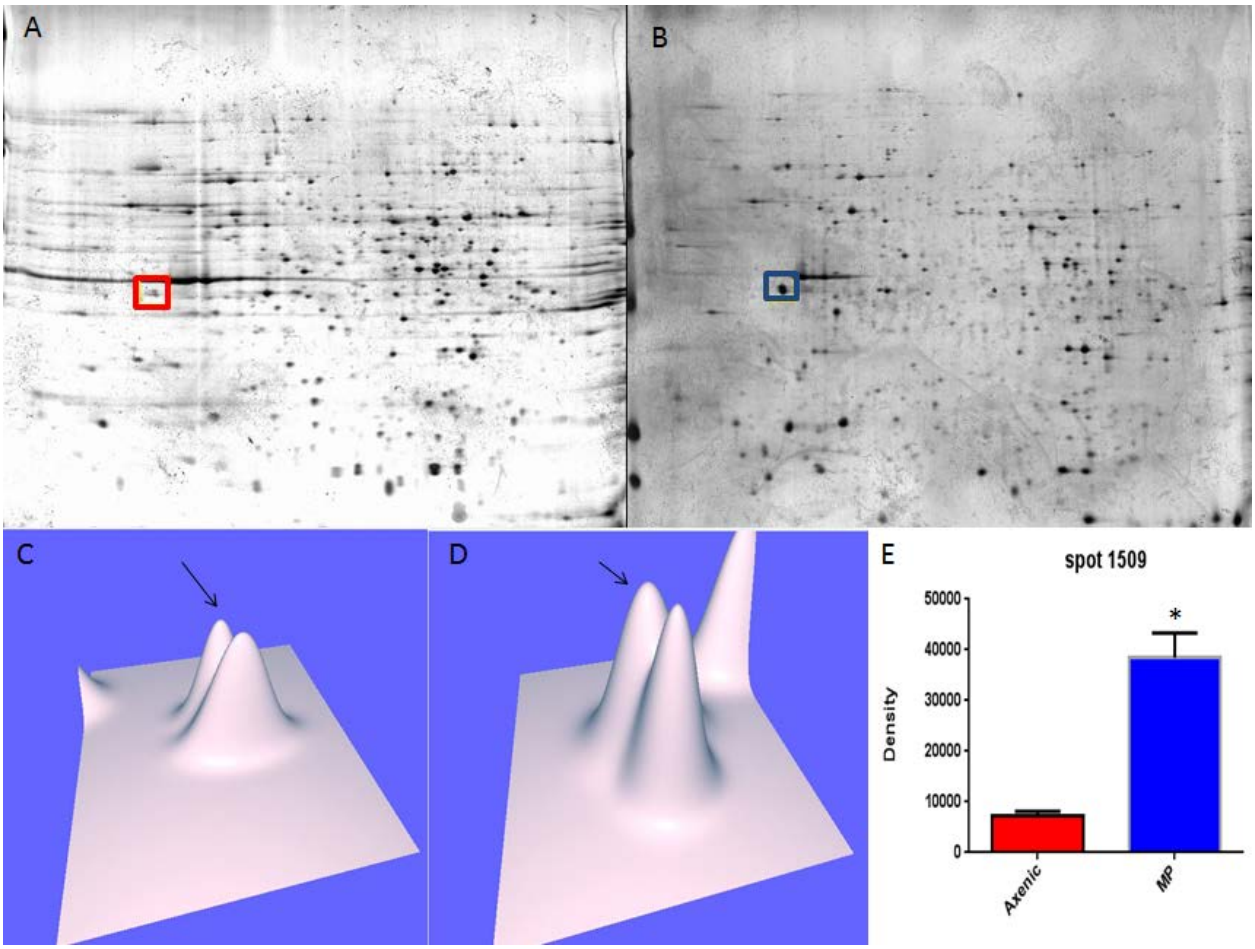

Figure 23. Analysis of spot 1509. The red box in Panel A and the blue box in Panel B show the location of the protein spot on two dimensional electrophoresis gels for axenically-grown (A) and mouse-passaged (B) *N. fowleri*, respectively. Panels C and D represent the three-dimensional rendering of the level of protein that is observed. Panel E is represented in a bar graph fashion and demonstrates the reproducibility of spot detection for each of the three gels that served as a composite for the master gel. Note that the density level of the protein doubletfor the given spot is elevated for the mouse-passaged three-dimensional image compared to the axenically-grown counterpart. The arrow designated the rear protein spot of each doublet. An analysis of the density values by Student's t-test indicates a p-value of 0.0004. Since this is below our significance level of 0.05, we can conclude that the density values have a statistically significant difference indicated by an asterisk (*).

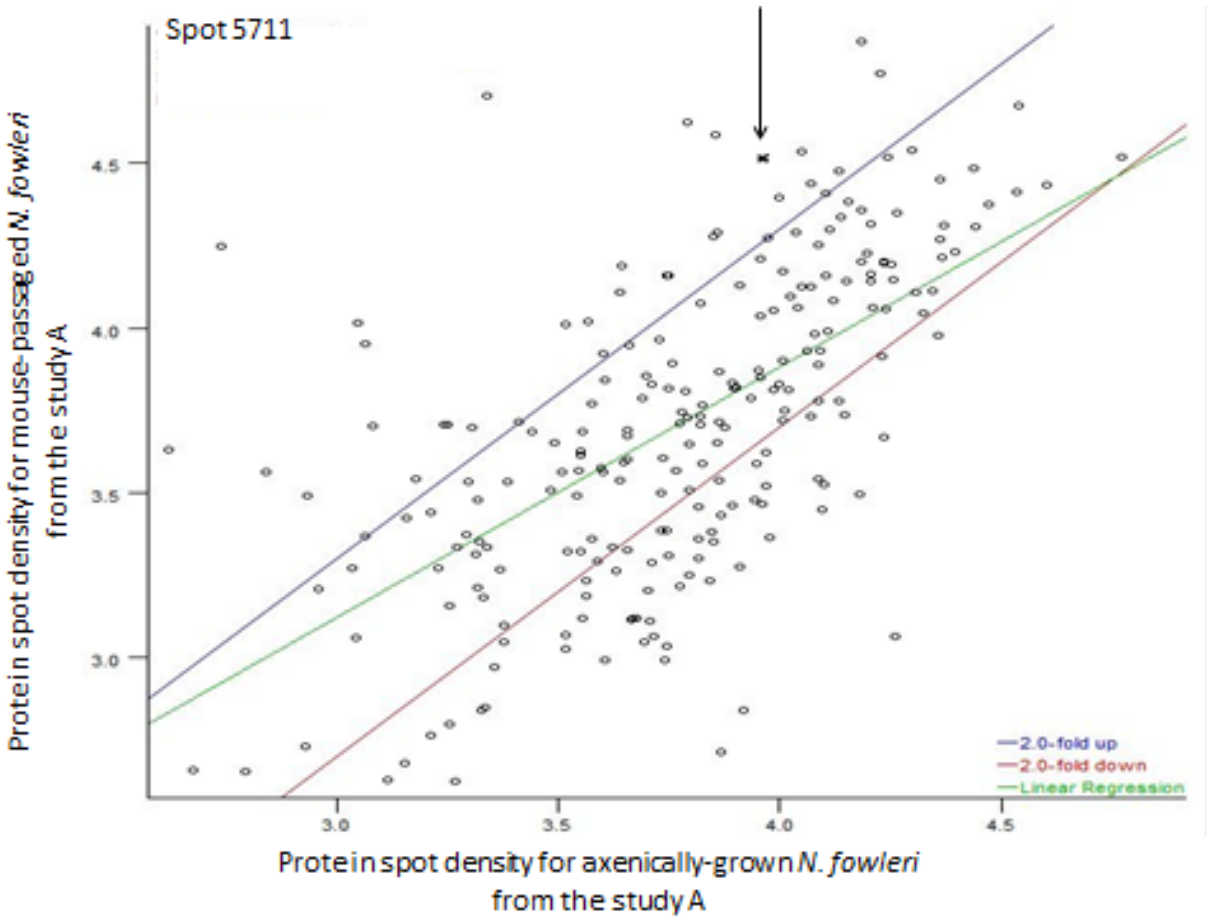

Figure 24. Scatter plot location of spot 5711. The arrow indicates the location of the protein in a density scatter plot mouse-passaged versus axenically-grown *N. fowleri*.

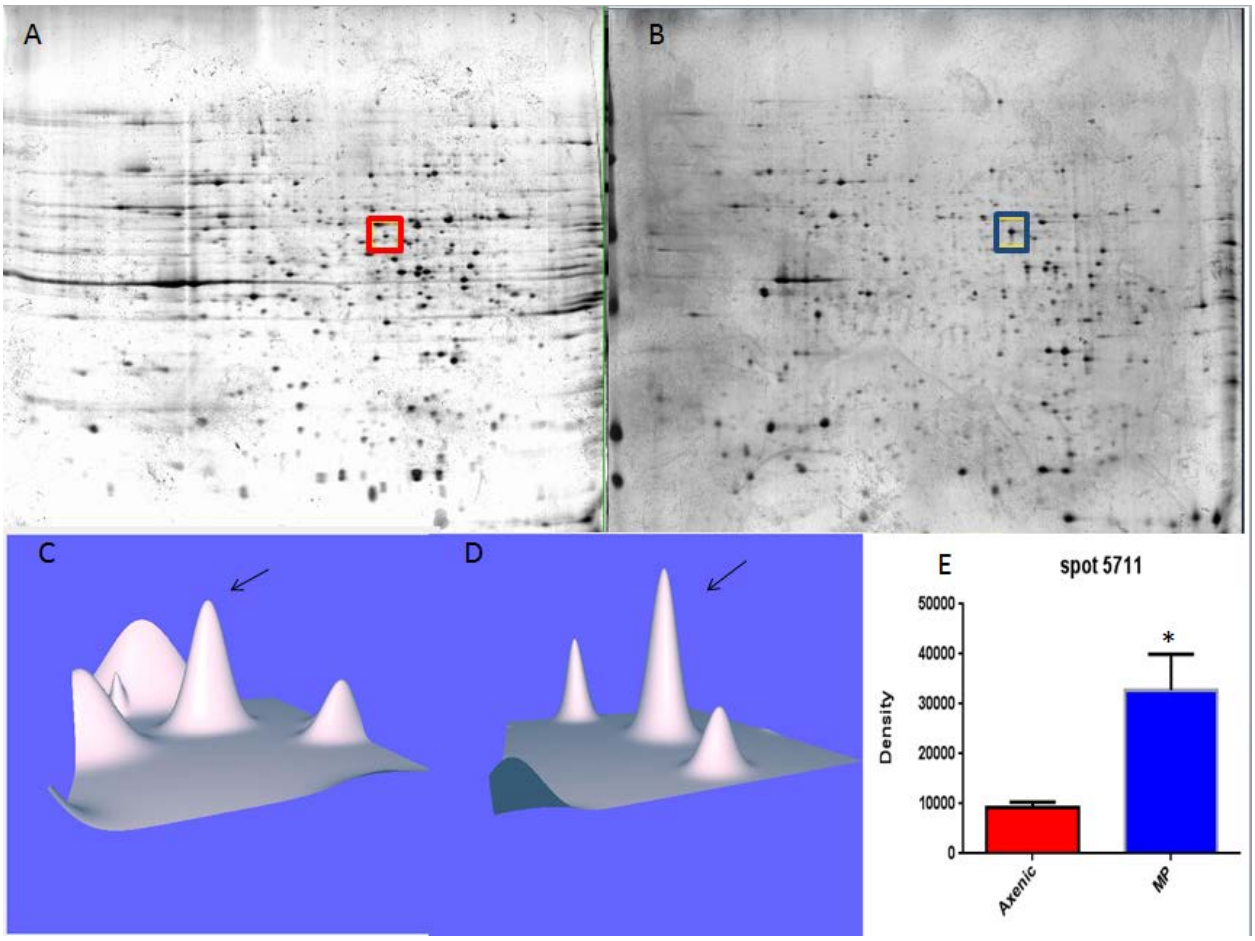

Figure 25. Analysis of spot 5711. The red box in Panel A and the blue box in Panel B show the location of the protein spot on two dimensional electrophoresis gels for axenically-grown (A) and mouse-passaged (B) *N. fowleri*, respectively. Panels C and D represent the three-dimensional rendering of the level of protein that is observed. Panel E is represented in a bar graph fashion and demonstrates the reproducibility of spot detection for each of the three gels that served as a composite for the master gel. Note that the density level of protein for the given spot is elevated for the mouse-passaged three-dimensional image compared to the axenically-grown counterpart. An analysis of the density values by Student's t-test indicates a p-value of 0.0048. Since this is below our significance level of 0.05, we can conclude that the density values have a statistically significant difference indicated by an asterisk (*).

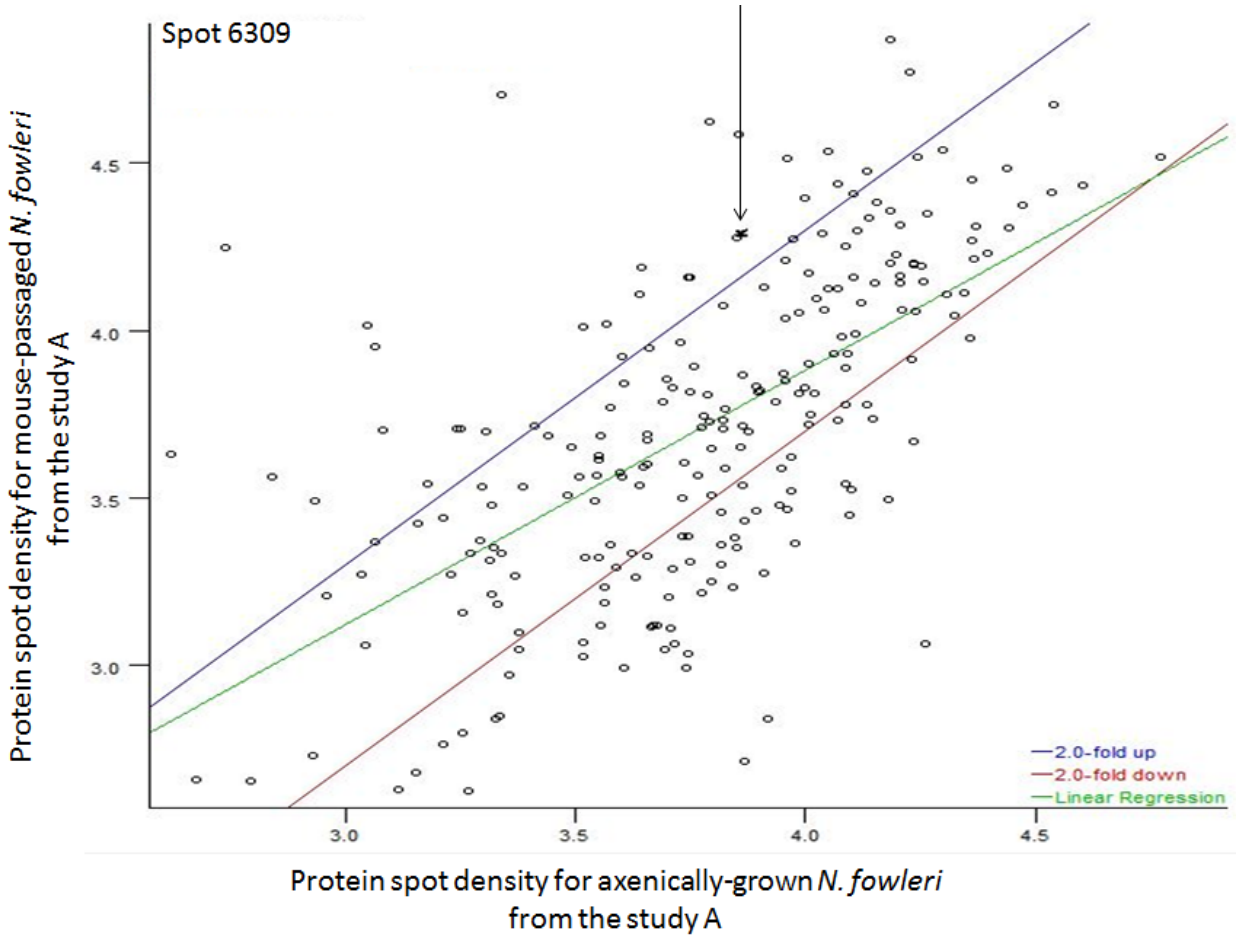

Figure 26. Scatter plot location of spot 6309. The arrow indicates the location of the protein in a density scatter plot for mouse-passaged versus axenically-grown *N. fowleri*.

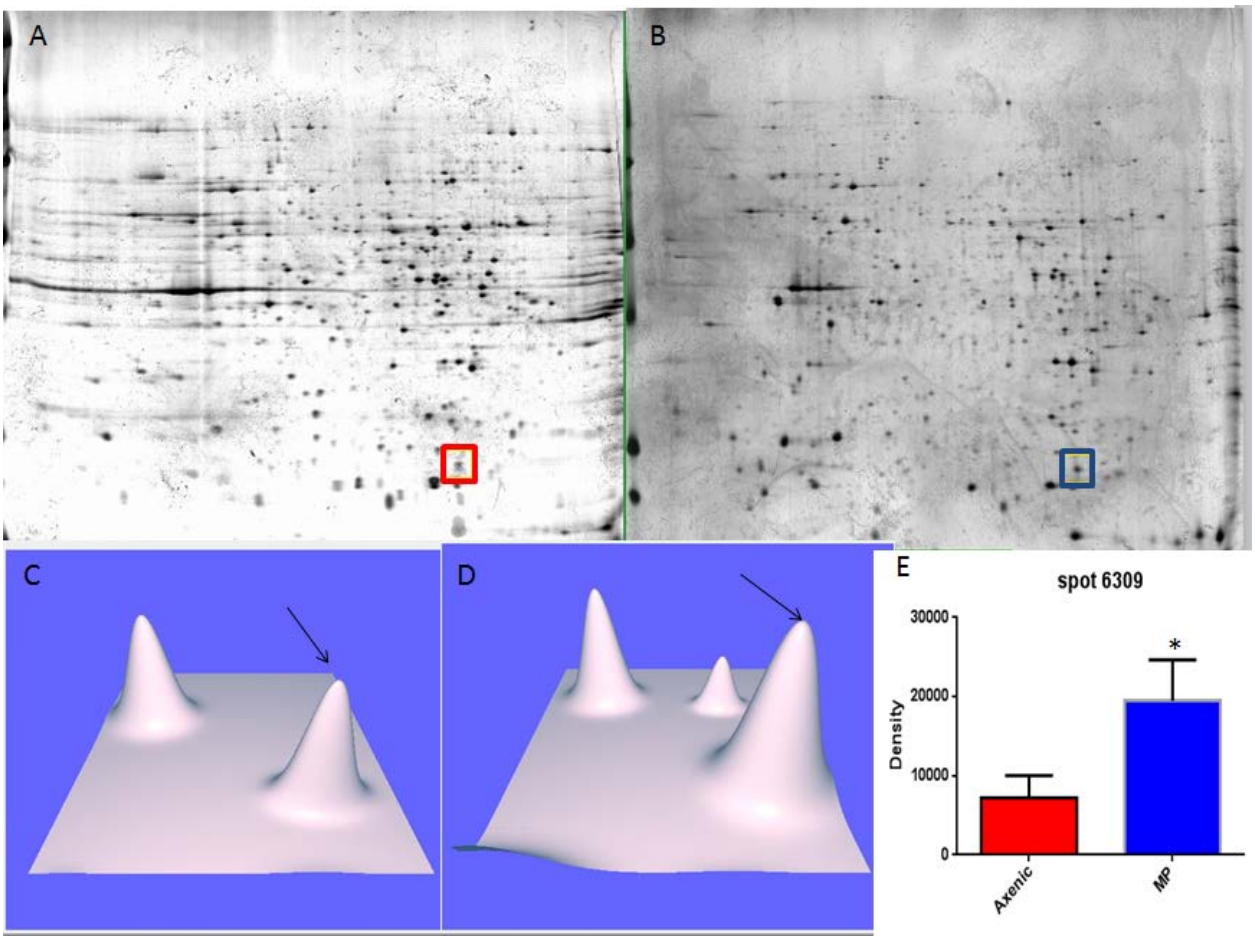

Figure 27. Analysis of spot 6309. . The red box in Panel A and the blue box in Panel B show the location of the protein spot on two-dimensional electrophoresis gels for both axenically-rown (A) and mouse-passaged (B) *N. fowleri*, respectively. Panels C and D represent the three-dimensional rendering of the level of protein that is observed. Panel E is represented in a bar graph fashion and demonstrates the reproducibility of spot detection for each of the three gels that served as a composite for the master gel. Note that the density level of protein for the given spot is elevated for the mouse- passaged three-dimensional image compared to the axenically-grown counterpart. Also note that a smaller protein spot is located to the left rear of the mouse-passaged panel shown. An analysis of the density values by Student's t-test indicates a p-value of 0.0223. Since this is below our significance level of 0.05, we can conclude that the density values have a statistically significant difference indicated by an asterisk (*).

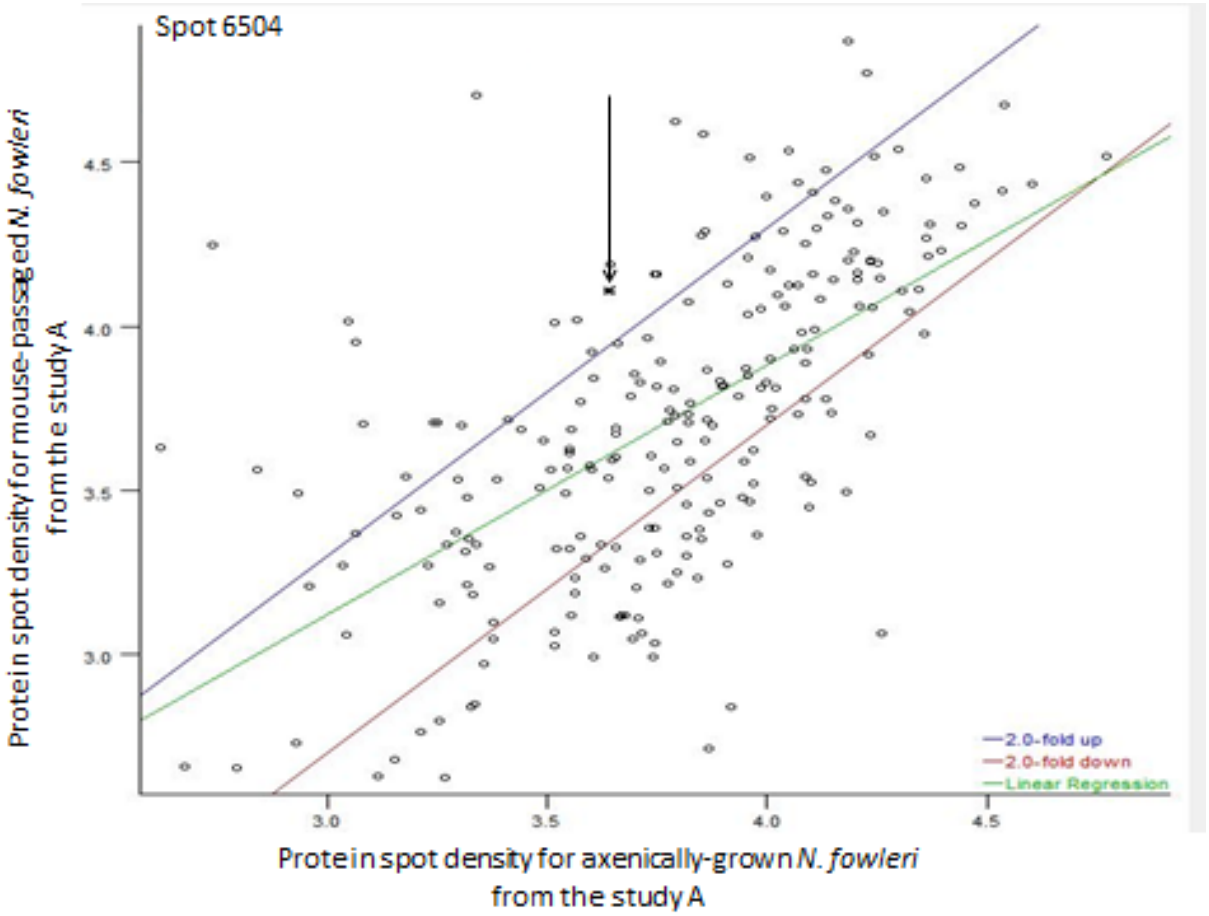

Figure 28. Scatter plot location of spot 6504. The arrow indicates the location of the protein in a density scatter plot for mouse-passaged versus axenically-grown *N. fowleri*.

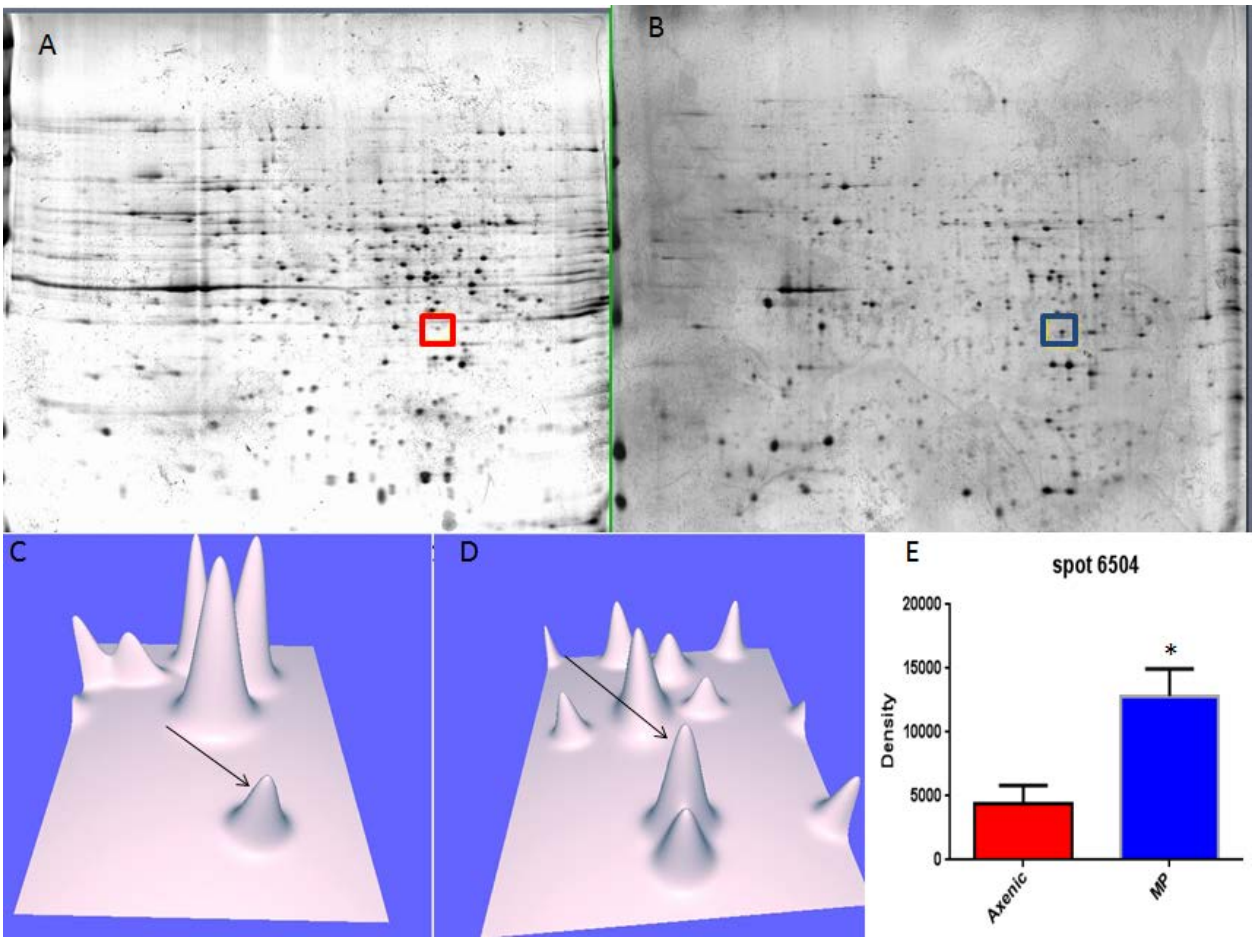

Figure 29. Analysis of spot 6504. . The red box in Panel A and the blue box in Panel B show the location of the protein on two-dimensional electrophoresis gels for both axenically-grown (A) and mouse-passaged (B) *N. fowleri*, respectively. Panels C and D represent the three-dimensional rendering of the level of protein that is observed. A differential pattern of protein spots is apparent for the axenically-grown versus mouse-passaged samples. Panel E is represented in a bar graph fashion and demonstrates the reproducibility of spot detection for each of the three gels that served as a composite for the master gel. Note that the density level of protein for the given spot is elevated for the mouse-passaged three-dimensional image compare to the axenically-grown counterpart. An analysis of the density values by Student's t-test indicates a p-value of 0.0047. Since this is below our significance level of 0.05, we can conclude that the density values have a statistically significant difference indicated by an asterisk (*).

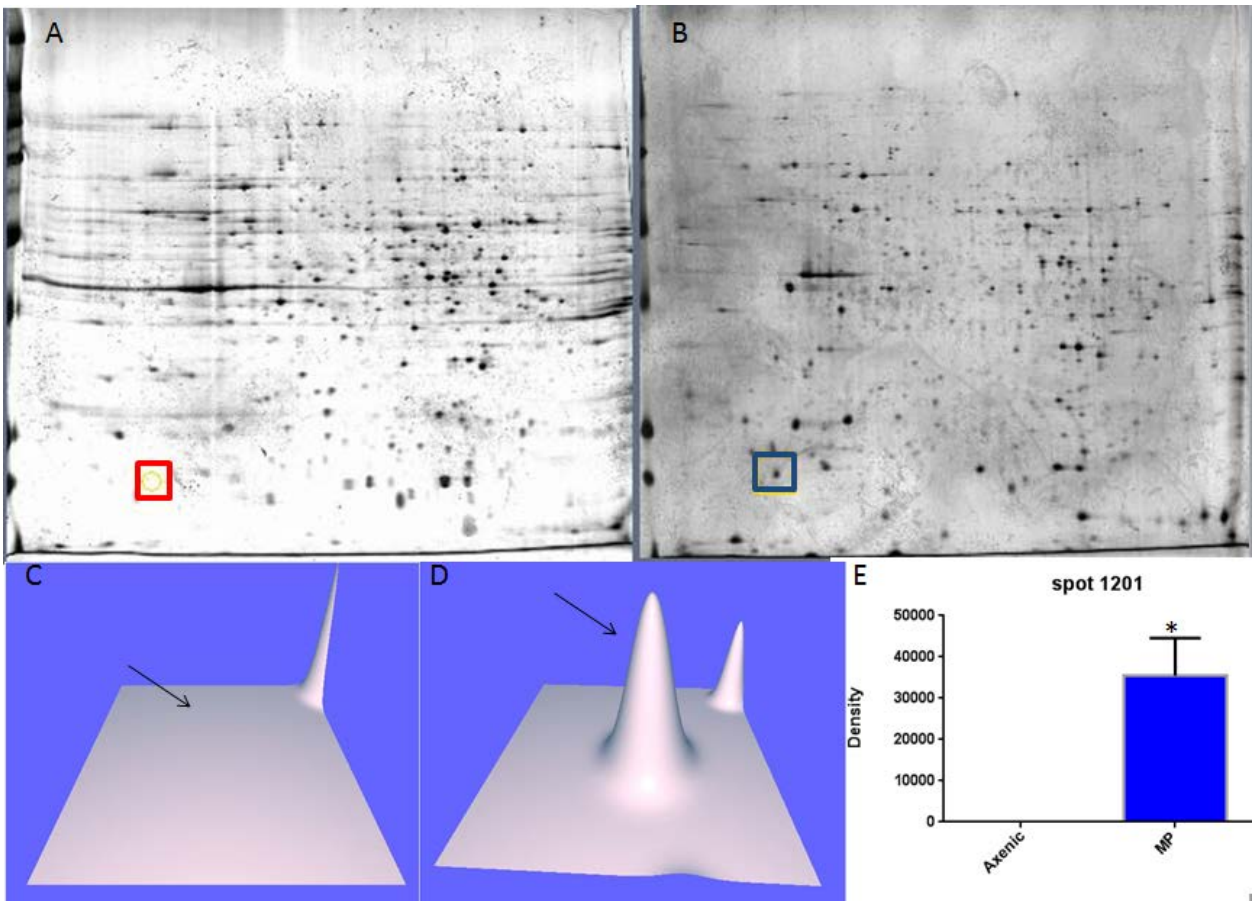

Figure 30. Analysis of Spot 1201. In Panel A, the red box is showing the theoretical area of the protein spot for axenically-grown *N. fowleri* (A) in the representative two-dimensional electrophoresis gel. The blue box shown in Panel B shows the location of the protein spot on the representative two-dimensional electrophoresis gel for mouse- passaged *N. fowleri* (B). Panels C and D represent the three-dimensional rendering of the level of protein that is observed. Panel E is represented in a bar graph fashion and demonstrates the reproducibility of spot detection for each of the three gels that served as a composite for the master gel. Note that the density level of protein for the mouse-passaged is observed, but the protein density level is not observed for the axenically-grown counterpart. An analysis of the density values by Student's t-test indicates a p-value of 0.0025. Since this is below our significance level of 0.05, we can conclude that the density values have a statistically significant difference indicated by an asterisk (*).

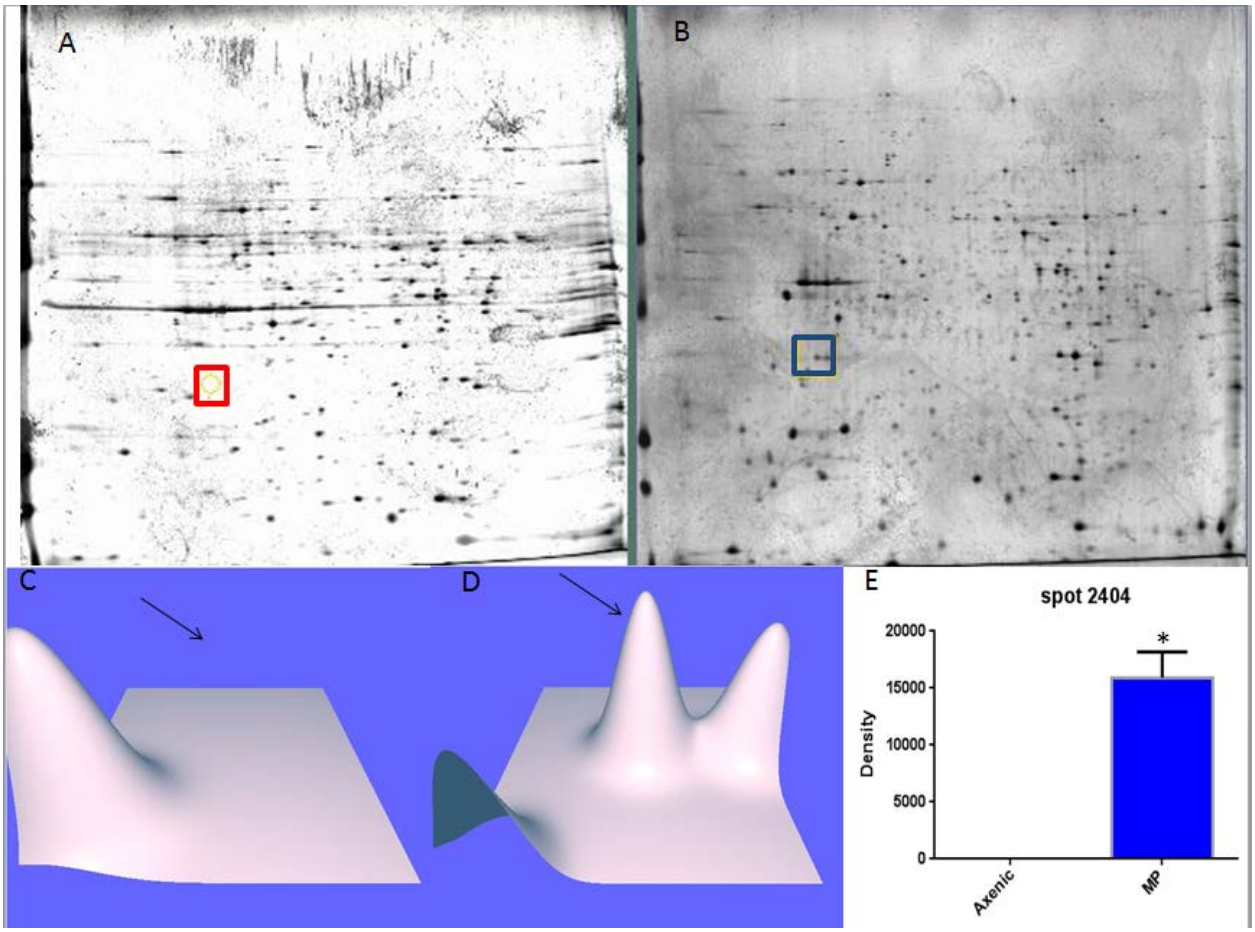

Figure 31. Analysis of Spot 2404. In Panel A, the red box is showing the theoretical area of the protein spot for axenically-grown *N. fowleri* (A) in the representative two-dimensional electrophoresis gel. The blue box shown in Panel B shows the location of the protein spot on the representative two-dimensional electrophoresis gel for mouse- passaged *N. fowleri* (B). Panels C and D represent the three-dimensional rendering of the level of protein that is observed. Panel E is represented in a bar graph fashion and demonstrates the reproducibility of spot detection for each of the three gels that served as a composite for the master gel. Note that the density level of protein for the mouse-passaged is observed, but the protein density level is not observed for the axenically-grown counterpart. An analysis of the density values by Student's t-test indicates a p-value of 0.0003. Since this is below our significance level of 0.05, we can conclude that the density values have a statistically significant difference indicated by an asterisk (*).

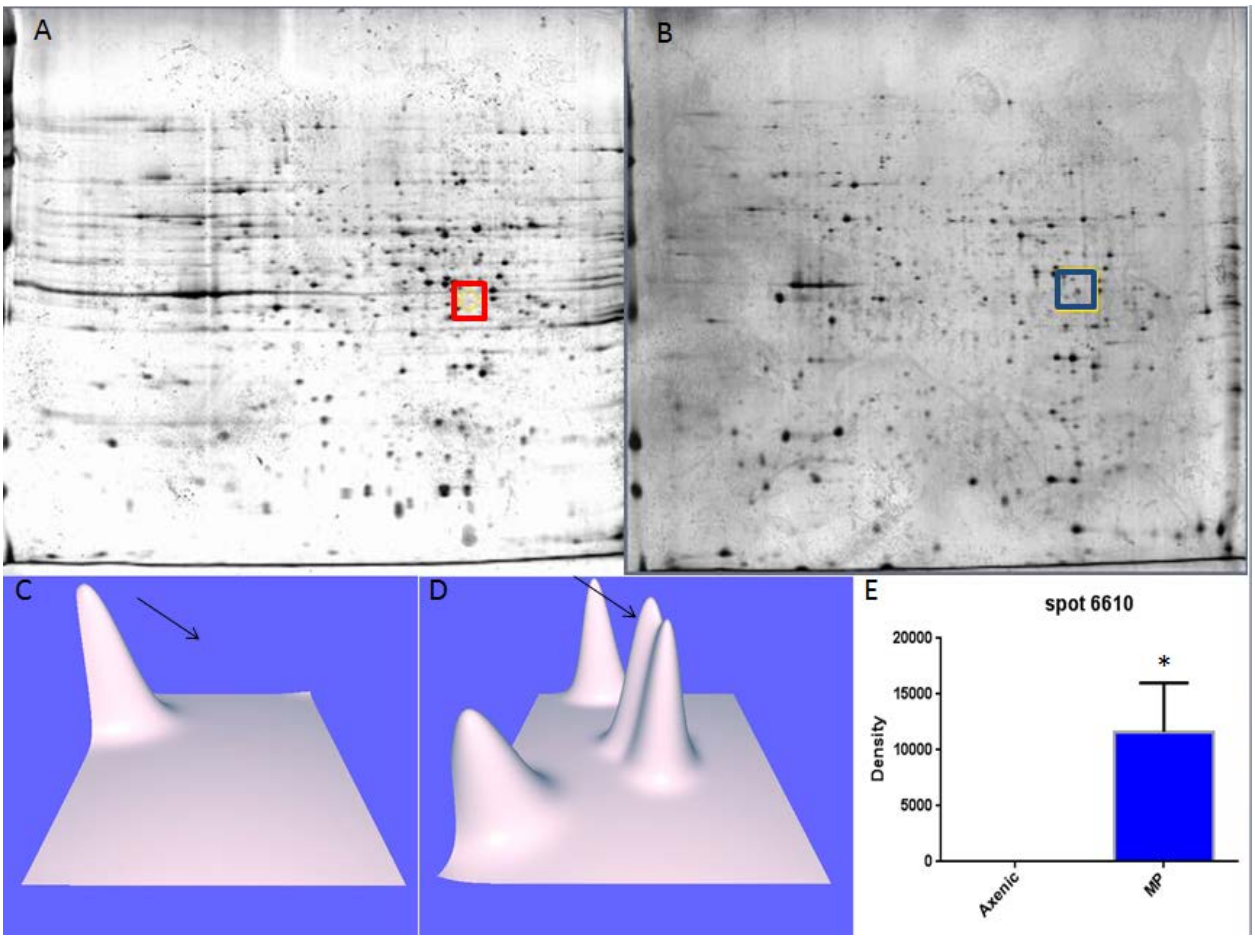

Figure 32. Analysis of Spot 6610. In Panel A, the red box is showing the theoretical area of the protein spot for axenically-grown *N. fowleri* (A) in the representative two-dimensional electrophoresis gel. The blue box shown in Panel B shows the location of the protein spot on the representative two-dimensional electrophoresis gel for mouse- passaged *N. fowleri* (B). Panels C and D represent the three-dimensional rendering of the level of protein that is observed. Panel E is represented in a bar graph fashion and demonstrates the reproducibility of spot detection for each of the three gels that served as a composite for the master gel. Note that the density level of protein for the mouse-passaged is observed, but the protein density level is not observed for the axenically-grown counterpart. An analysis of the density values by Student's t-test indicates a p-value of 0.0101. Since this is below our significance level of 0.05, we can conclude that the density values have a statistically significant difference indicated by an asterisk (*).

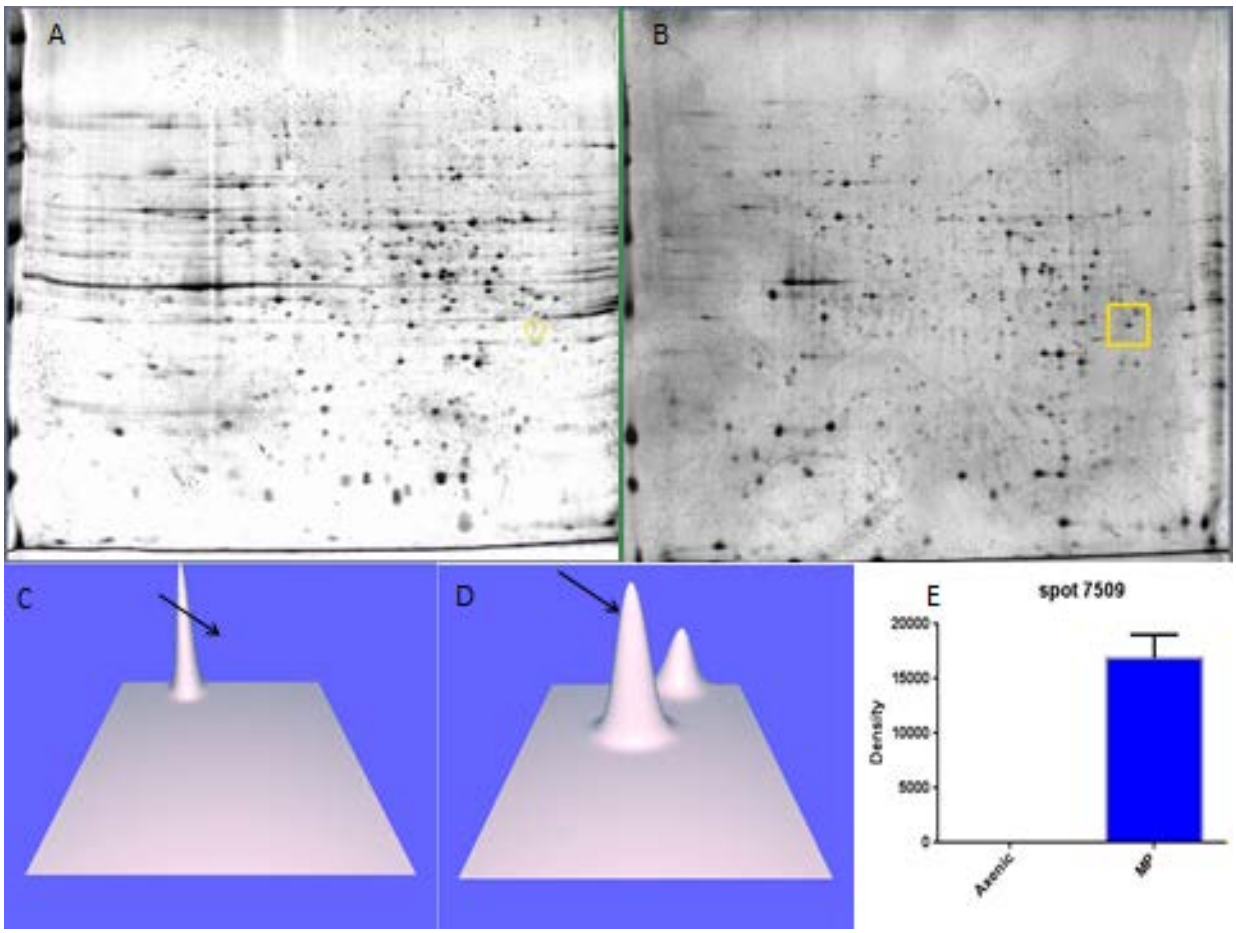

Figure 33. Analysis of Spot 7509. In Panel A, the red box is showing the theoretical area of the protein spot for axenically-grown *N. fowleri* (A) in the representative two-dimensional electrophoresis gel. The blue box shown in Panel B shows the location of the protein spot on the representative two-dimensional electrophoresis gel for mouse- passaged *N. fowleri* (B). Panels C and D represent the three-dimensional rendering of the level of protein that is observed. Panel E is represented in a bar graph fashion and demonstrates the reproducibility of spot detection for each of the three gels that served as a composite for the master gel. Note that the density level of protein for the mouse-passaged is observed, but the protein density level is not observed for the axenically-grown counterpart. An analysis of the density values by Student's t-test indicates a p-value of 0.0002. Since this is below our significance level of 0.05, we can conclude that the density values have a statistically significant difference indicated by an asterisk (*).

Spot #	Approximate Cartesian Coordinates on the map (rMw, pI)
0006	(17.5, 5.4)
1207	(23.0, 5.9)
1509	(41.0, 5.7)
5711	(50.9, 7.0)
6309	(23.1, 7.3)
6504	(36.9, 7.2)
1201	(19.9, 5.5)
2404	(32.0, 5.8)
6610	(41.4, 7.3)
7509	(36.0, 7.7)

Table 3. Cartesian coordinates for spots of interest. The Cartesian coordinates were generated using the representative two-dimensional electrophoresis gels for mouse-passaged and axenically-grown *N. fowleri* for the protein spots that are differentially expressed. As for the proteins spots that were only found in 2-D gels for mouse passaged *N. fowleri*, only the replicated 2-D gels for mouse passaged *N. fowleri* were used.

DISCUSSION

Naegleria fowleri (*N. fowleri*) is the only species of the genus *Naegleria* that has been isolated from fatal CNS infections in humans (Martinez, 1985; Yoder et al., 2004). Two other species of *Naegleria*, *N. australiensis* and *N. italica*, have been shown to lyse tissue culture cells in vitro and are pathogenic in experimental animals but have not been associated with disease in humans (Marciano-Cabral, F.M., 1986; De Jonckheere, 2004). Primary Amoebic Meningoencephalitis (PAM) is caused by *N. fowleri* and has been observed in many parts of the world (Brown, T. J. 1983 , Carter, R.F. 1968, Craun, G.F. 2005). Typical infection occurs through the nasal passage and the prognosis of infection is very low (Center for Disease Control and Prevention Nov. 9. 2012). In the natural environment, *N. fowleri* can be found in different morphological forms depending on ambient conditions, but they can also be grouped into two strains or states: highly-pathogenic and weakly-pathogenic. In the literature it has been reported that mouse-passaged *N. fowleri* correlates to the pathogenic state while axenically-grown *N. fowleri* correlates to the less pathogenic state (De Jonckheere,J. 1977). The objective of the first phase of this study was to determine whether the *N. fowleri* used in our study correlated with being in a pathogenic state versus a less-pathogenic state. In order to achieve this objective, ID_{50} assays were performed. Through ID_{50} analysis it was determined that the ID_{50} for mouse-passaged *N. fowleri* was 200 ID_{50} units/10 µl of intranasal inoculum while that for the less pathogenic axenically-grown *N. fowleri* was 11,857 ID_{50} units/10 µl of intranasal inoculum. Thus, a 1.77 fold logarithmic logarithmic difference was obtained in ID_{50} for mouse-passaged versus axenically-grown amebae. The mouse-passaged and axenically-grown amebae were screened for potential residual contaminating brain tissue of bacteria by transmission electron microscopy and bacterial colony formation. No evidence of the presence of bacteria or mouse brain tissue debris

was obtained. These assessments were required so as to minimize confounding interpretation of protein spots in subsequent proteomic analysis as representing amebic gene expression products. Finally, amebae were screened before advancing in our research to make sure that they were in an amebic state. This was important to avoid misinterpretation of differential protein profiles as due to assumption of a flagellate or cyst state rather than representing amebic forms associated with the mouse-passaged highly-pathogenic versus axenically-grown weakly-pathogenic states.

The mouse-passaged and axenically-grown *N. fowleri* then were subjected to a high resolution proteomic analysis to establish a proteomic template for each of the variant pathogenic states of *N. fowleri*. Proteins were separated in the first dimension in a pH gradient that ranged from pH 5-8 and in the second dimension by 10% SDS-PAGE that allowed for a relative molecular range of separation of 10 kDa – 160 kDa. Thus, a proteomic profile for highly basic proteins, or proteins that have a high isoelectric point and tend to be positively charged at physiological pH (7.4), was not obtained. The non-encompassed basic proteins would consist of highly-positive proteins that exhibit DNA –binding properties. Similarly, highly acidic proteins, or proteins that have a low isoelectric point and that tend to be negatively charged at physiological pH (7.4), were not included. Finally, proteins for which the relative molecular weight was less that 10 kDa were excluded. Nevertheless, the proteomic profile that was obtained with the pH5-8 and relative molecular weight range of 10kDa to 160 kDa included approximately 230 protein species and contained a subset of proteins that allowed for the generation of a distinctive discriminative protein coordinate profile for mouse-passaged versus axenically-grown *N. fowleri*. Thus, a proteomic "finger print" was generated for the mouse-passaged versus axenically-grown *N. fowleri*, although the experimental design applied to the present study did not allow for establishing a functional linkage between these amebae being

highly-pathogenic versus weakly-pathogenic. Scatter plot analysis using pair-wise Student's *t*-tests was employed as a basis for identification of differentially expressed proteins in mouse-passaged versus axenically-grown *N. fowleri*. A best-fit line was generated for each protein population master gel composite from mouse-passaged versus axenically-grown amebae. Protein spots that were located outside of two standard deviations from the best-fit line were considered as differentially expressed. Emphasis was placed on identifying novel expressed or differentially up regulated proteins for mouse-passaged versus axenically-grown amebae in order to garner insight as to protein species that could be linked to the highly-pathogenic state. Proteins thus identified proteins would serve as candidates for subsequent mass spectrometry analysis. The proteins that are within two standard deviations from the best-fit line in the Scatter Plot for mouse-passaged versus axenically-grown amebae are considered as expressed at comparable levels in mouse-passaged and axenically-grown amebae. Proteins localized at two standard deviations below the best fit line have a 95% likelihood of being associated with axenically-grown amebae. In contrast, proteins that are localized above two standard deviations from the best-fit line in the Scatter plot have a 95% likelihood of being associated with mouse-passaged amebae. Of the 230 proteins present in comparative master gels of mouse-passaged versus axenically-grown amebae, six proteins were consistently up-regulated for mouse-passaged of *N. fowleri* and were two-standard deviations above the best-fit line and within a 95% conference interval. These were located in the upper right quadrant of the scatter plot that is indicative of sufficient density level to allow for mass spectrometry analysis.

Two-dimensional gel electrophoresis in concert with mass spectrometry and bioinformatics are the key components of current proteomics technology (Beranova-Giorgianni, Sarka 2003). Protein visualization on two-dimensional electrophoresis gels is the key feature of

two dimensional gel electrophoresis analyses. Countless staining procedures have been reported in the literature and can be divided into colorimetry and flurescence (Miller, I. 2006). Coomassie Brilliant Blue (CBB) and silver nitrate (SN) are the most frequently used visible stains. CBB is very popular and is compatible with mass spectrometry (Lin, J.F. 2008). Silver staining, ever since it was first introduced for protein detection in 1979 (Merril, C.R. 1979), has been the most sensitive nonradioactive method for protein visualization, enabling protein spots of just under 0.1 ng to be detected. The high sensitivity of silver staining not only lowers the amount of protein needed for proteomic analysis, but also facilitates the identification of low-abundance protein. Furthermore, when mass-spectrometry-compatible silver staining procedures are used, the protein spots can be visualized without special scanners and subsequently excised from the gel for further mass spectrometry identification. The Vorum SN staining method has been found to give a very clean background and a very clear contrast out of all of the SN staining methods cited in literature and is sensitive to about 1ng of protein (Vorum 2004, Lin, J.F. 2008). This staining method only affects 10% of the total protein population and therefore is compatible with mass spectrometry analysis. However, between any two gels, there is always some variation. To address this problem, two-dimensional difference in gel technology (2D-DIGE) has been employed for a further differential protein expression analyses. The main attributes of DIGE are the capability to resolve multiple samples on one gel, and the use of an internal standard for cross-gel normalization. The internal standard is critical for the removal of gel to gel variation, accurate quantitation and reproducibility (Alban, A. 2003). In the present study, 2D-DIGE was used to provide a general confirmation that protein expression profiles for mouse-passaged versus axenically-grown *N. fowleri* are distinctive.

It is important to understand that the statistical analysis using two-dimensional electrophoresis gels includes some inaccuracies. The Y-axis intercept of the Scatter plot can but very difficult to be extrapolated to exactly zero. Multiple gels were analyzed in order to address for intra-experimental and inter-experimental variation due to sample loading errors or possible protein degradation. Protein degradation was minimized by aliquoting whole cell lysates and storing them at -80C until use and by addition of a protease inhibitor- cocktail to each sample. To address for loading errors, multiple gels of the same whole lysate (individually thawed) were created. The summation of these discrepancies will ultimately result in a shift of the y-axis to a number other than zero. Finally, as an intra-experimental control, when constructing a master gel from component individual gels, an R-value of 0.90 was observed. That is, the closer the correlation values are to 1, the better the fit for the regression line to the data values. .

In the present study, initial insight was obtained regarding protein gene products that are associated with the highly-pathogenic state of *N. fowleri*. The protein spots that were identified in this study include both differentially expressed proteins found in mouse-passaged versus axenically-grown amebae as well as proteins that are expressed de *novo* in mouse-passage amebae. . The present studies are correlative in that mouse-passaged amebae were shown to be relatively more pathogenic in mice based on exhibiting a low ID_{50} as compared with the axenically-grown amebae. Nevertheless, they serve as a basis for identification of candidate proteins that will be analyzed further by mass spectrometry to allow for their identification. Such identification then will be instrumental in the conduct of studies for their selective neutralization or knockdown pursuant to assessment of whether such action ablates the pathogenicity of mouse-passaged N. fowleri. PAM is typically associated with younger patients and is found to be very difficult to detect and treat (Center for Disease Control and Prevention Nov. 9. 2012). Therefore,

identification of a protein linked functionally to the highly-pathogenic state may provide novel insights into therapeutic regimens that can be applied to treat this disease.

The proteins that have been identified have potential to serve as therapeutic targets for ablating untoward effects linked to infection with highly-pathogenic *N. fowleri*. Thus, not only can drugs be developed that target these proteins, but also such proteins may serve as diagnostic markers for differentiating highly-pathogenic versus weakly-pathogenic *N. fowleri*.

LITERATURE CITED

Alban, A., David, S. O., Bjorkesten, L., Andersson, C., Sloge, E., Lewis, S., et al. (2003). A novel experimental design for comparative two-dimensional gel analysis: Two-dimensional difference gel electrophoresis incorporating a pooled internal standard. *Proteomics, 3*(1), 36-44.

Beranova-Giorgianni, S. (2003). Proteome analysis by two-dimensional gel electrophoresis and mass spectrometry: Strengths and limitations. *TrAC Trends in Analytical Chemistry, 22*(5), 273-281.

Brown, T. J., Cursons, R. T. M., Keys, E. A., Marks, M., & Miles, M. (1983). The occurrence and distribution of pathogenic free-living amoebae in thermal areas of the north island of new zealand. *New Zealand Journal of Marine and Freshwater Research, 17*(1)

Butt, C. G. (1966). Primary amebic meningoencephalitis. *The New England Journal of Medicine, 274*(26), 1473-1476.

Butt, C. G., Baro, C., & Knorr, R. W. (1968). Naegleria (sp.) identified in amebic encephalitis. *American Journal of Clinical Pathology, 50*(5), 568-574.

Carter, R. F. (1968). Primary amoebic meningo-encephalitis: Clinical, pathological and epidemiological features of six fatal cases. *The Journal of Pathology and Bacteriology, 96*(1), 1-25.

Carter, R. F. (1970). Description of a naegleria sp. isolated from two cases of primary amoebic meningo-encephalitis, and of the experimental pathological changes induced by it. *The Journal of Pathology,100*(4), 217-244.

Carter, R. F. (1972). Primary amoebic meningo-encephalitis. an appraisal of present knowledge. *Transactions of the Royal Society of Tropical Medicine and Hygiene, 66*(2), 193-213.

Center for Disease Control and Prevention. (Nov. 9. 2012). *Naegleria fowleri - Primary amebic meningoencephalitis.* Retrieved Mar. 5., 2013, from http://www.cdc.gov/parasites/naegleria/pathogen.html

Cerva, L., & Novak, K. (1968). Amoebic meningoencephalitis: 16 fatalities. *Science (New York, N.Y.), 160*(3823), 92.

Chang, S. L. (1978). Resistance of pathogenic naegleria to some common physical and chemical agents. *Applied and Environmental Microbiology, 35*(2), 368-375.

Craun, G. F., Calderon, R. L., & Craun, M. F. (2005). Outbreaks associated with recreational water in the united states. *International Journal of Environmental Health Research, 15*(4), 243-262.

Culbertson, C. G. (1971). The pathogenicity of soil amebas. *Annual Review of Microbiology, 25*, 231-254.

CULBERTSON, C. G., SMITH, J. W., & MINNER, J. R. (1958). Acanthamoeba: Observations on animal pathogenicity. *Science (New York, N.Y.), 127*(3313), 1506.

da Rocha-Azevedo, B., Tanowitz, H. B., & Marciano-Cabral, F. (2009). Diagnosis of infections caused by pathogenic free-living amoebae. *Interdisciplinary Perspectives on Infectious Diseases, 2009*, 251406.

De Jonckheere, J. (1977). Use of an axenic medium for differentiation between pathogenic and nonpathogenic naegleria fowleri isolates. *Applied and Environmental Microbiology, 33*(4), 751-757.

De Jonckheere, J. F. (2004). Molecular definition and the ubiquity of species in the genus naegleria. *Protist, 155*(1), 89-103.

Fowler, M., & Carter, R. F. (1965). Acute pyogenic meningitis probably due to acanthamoeba sp.: A preliminary report. *British Medical Journal, 2*(5464), 740-742.

Gustavo dos Santos, N. (1970). Fatal primary amebic meningoencephalitis. A retrospective study in richmond, virginia. *American Journal of Clinical Pathology, 54*(5), 737-742.

Jamerson, M., Remmers, K., Cabral, G., & Marciano-Cabral, F. (2009). Survey for the presence of naegleria fowleri amebae in lake water used to cool reactors at a nuclear power generating plant.*Parasitology Research, 104*(5), 969-978.

John, D. T. (1982). Primary amebic meningoencephalitis and the biology of naegleria fowleri. *Annual Review of Microbiology, 36*, 101-123.

John, D. T., Cole, T. B.,Jr, & Bruner, R. A. (1985). Amebostomes of naegleria fowleri. *The Journal of Protozoology, 32*(1), 12-19.

John, D. T., Cole, T. B.,Jr, & Marciano-Cabral, F. M. (1984). Sucker-like structures on the pathogenic amoeba naegleria fowleri. *Applied and Environmental Microbiology, 47*(1), 12-14.

John, D. T., & John, R. A. (1989). Cytopathogenicity of naegleria fowleri in mammalian cell cultures. *Parasitology Research, 76*(1), 20-25.

Kidney, D. D., & Kim, S. H. (1998). CNS infections with free-living amebas: Neuroimaging findings. *AJR.American Journal of Roentgenology, 171*(3), 809-812.

Lawande, R. V., Abraham, S. N., John, I., & Egler, L. J. (1979). Recovery of soil amebas from the nasal passages of children during the dusty harmattan period in zaria. *American Journal of Clinical Pathology, 71*(2), 201-203.

Lin, J. F., Chen, Q. X., Tian, H. Y., Gao, X., Yu, M. L., Xu, G. J., et al. (2008). Stain efficiency and MALDI-TOF MS compatibility of seven visible staining procedures. *Analytical and Bioanalytical Chemistry,390*(7), 1765-1773.

Marciano-Cabral, F. (1988). Biology of naegleria spp. *Microbiological Reviews, 52*(1), 114-133.

Marciano-Cabral, F., & Cabral, G. A. (2007). The immune response to naegleria fowleri amebae and pathogenesis of infection. *FEMS Immunology and Medical Microbiology, 51*(2), 243-259.

Marciano-Cabral, F. M., & Fulford, D. E. (1986). Cytopathology of pathogenic and nonpathogenic naegleria species for cultured rat neuroblastoma cells. *Applied and Environmental Microbiology, 51*(5), 1133-1137.

Martinez, A. J. (1985). *Free-living amoebas; natural history, prevention, diagnosis, pathology and treatment of disease*. Boca Raton, Florida: CRC Press.

Martinez, A. J., dos Santos Neto, J. G., Nelson, E. C., Stamm, W. P., & Willaert, E. (1977). Primary amebic meningoencephalitis. *Pathology Annual, 12 Pt 2*, 225-250.

Martinez, A. J., & Kasprzak, W. (1980). Pathogenic free-living amoebae - a review. [Patogenne Pelzaki wolnozyjace - Przeglad] *Wiadomosci Parazytologiczne, 26*(6), 495-522.

Martinez, A. J., & Visvesvara, G. S. (1991). Laboratory diagnosis of pathogenic free-living amoebas: Naegleria, acanthamoeba, and leptomyxid. *Clinics in Laboratory Medicine, 11*(4), 861-872.

Martinez, A. J., & Visvesvara, G. S. (1997). Free-living, amphizoic and opportunistic amebas. *Brain Pathology (Zurich, Switzerland), 7*(1), 583-598.

Merril, C. R., Switzer, R. C., & Van Keuren, M. L. (1979). Trace polypeptides in cellular extracts and human body fluids detected by two-dimensional electrophoresis and a highly sensitive silver stain.*Proceedings of the National Academy of Sciences of the United States of America, 76*(9), 4335-4339.

Miller, I., Crawford, J., & Gianazza, E. (2006). Protein stains for proteomic applications: Which, when, why? *Proteomics, 6*(20), 5385-5408.

Schumacher, D. J., Tien, R. D., & Lane, K. (1995). Neuroimaging findings in rare amebic infections of the central nervous system. *AJNR.American Journal of Neuroradiology, 16*(4 Suppl), 930-935.

Schuster, F. L. (2002). Cultivation of pathogenic and opportunistic free-living amebas. *Clinical Microbiology Reviews, 15*(3), 342-354.

Seidel, J. S., Harmatz, P., Visvesvara, G. S., Cohen, A., Edwards, J., & Turner, J. (1982). Successful treatment of primary amebic meningoencephalitis. *The New England Journal of Medicine, 306*(6), 346-348.

Sparagano, O., Drouet, E., Brebant, R., Manet, E., Denoyel, G. A., & Pernin, P. (1993). Use of monoclonal antibodies to distinguish pathogenic naegleria fowleri (cysts, trophozoites, or flagellate forms) from other naegleria species. *Journal of Clinical Microbiology, 31*(10), 2758-2763.

Unlu, M., Morgan, M. E., & Minden, J. S. (1997). Difference gel electrophoresis: A single gel method for detecting changes in protein extracts. *Electrophoresis, 18*(11), 2071-2077.

Vargas-Zepeda, J., Gomez-Alcala, A. V., Vasquez-Morales, J. A., Licea-Amaya, L., De Jonckheere, J. F., & Lares-Villa, F. (2005). Successful treatment of naegleria fowleri meningoencephalitis by using intravenous amphotericin B, fluconazole and rifampicin. *Archives of Medical Research, 36*(1), 83-86.

Vargas-Zepeda, J., Gomez-Alcala, A. V., Vasquez-Morales, J. A., Licea-Amaya, L., De Jonckheere, J. F., & Lares-Villa, F. (2005). Successful treatment of naegleria fowleri meningoencephalitis by using intravenous amphotericin B, fluconazole and rifampicin. *Archives of Medical Research, 36*(1), 83-86.

Visvesvara, G. S., Moura, H., & Schuster, F. L. (2007). Pathogenic and opportunistic free-living amoebae: Acanthamoeba spp., balamuthia mandrillaris, naegleria fowleri, and sappinia diploidea. *FEMS Immunology and Medical Microbiology, 50*(1), 1-26.

Vorum, H., Ostergaard, M., Hensechke, P., Enghild, J. J., Riazati, M., & Rice, G. E. (2004). Proteomic analysis of hyperoxia-induced responses in the human choriocarcinoma cell line JEG-3. *Proteomics, 4*(3), 861-867.

Whiteman, L. Y., & Marciano-Cabral, F. (1989). Resistance of highly pathogenic naegleria fowleri amoebae to complement-mediated lysis. *Infection and Immunity, 57*(12), 3869-3875.

Wong, M. M., Karr, S. L.,Jr., & Chow, C. K. (1977). Changes in the virulence of naegleria fowleri maintained in vitro. *The Journal of Parasitology, 63*(5), 872-878.

Yoder, J. S., Eddy, B. A., Visvesvara, G. S., Capewell, L., & Beach, M. J. (2010). The epidemiology of primary amoebic meningoencephalitis in the USA, 1962-2008. *Epidemiology and Infection, 138*(7), 968-975.

VITA

Hong Geun Park was born on January 23, 1987 in Seoul, South Korea. He attended West High School, Knoxville, Tennessee and Centreville High School, Centreville, Virginia. He received a Bachelor of Science degree in Biological Chemistry from the University of Virginia in 2009.